The RhoGEF ECT-2 is required for ventral enclosure during *C. elegans* embryogenesis

Yun Chen

A Thesis in the

Department of Biology

Presented in the Partial Fulfillment of the Requirements for the

Degree of Maters of Science (Biology) at

Concordia University

Montreal, Quebec, Canada

April 12, 2014

This is to certify that the thesis prepared

By: Yun Chen

Entitled: The RhoGEF ECT-2 is required in ventral enclosure during

                 C. elegans embryogenesis

and submitted in partial fulfillment of the requirements for the degree of

Master of Science (Biology)

complies with the regulations of the University and meets the accepted standards

with respect to originality and quality.

Signed by the final Examining Committee:

_____ Chair

Dr. Selvadurai Dayanandan

_____ External Examiner

Dr. Malcolm Whiteway

_____ Examiner

Dr. Catherine Bachewich

_____ Examiner

Dr. Vladimir Titorenko

_____ Supervisor

Dr. Alisa Piekny

Approved by   _____

                          Dr. Selvadurai Dayanandan, Graduate Program Director

April 08, 2014   _____

                          Joanne Locke, Interim Dean of Faculty

Abstract

The RhoGEF ECT-2 is required in ventral enclosure during *C. elegans* embryogenesis

Yun Chen

Tissue morphogenesis is crucial for the development of metazoans. *C. elegans*, is a model system for studying tissue morphogenesis, as there are many genetic tools available, and embryos are amenable to microscopy. We study ventral enclosure, which is the process where ventral epidermal cells migrate to enclose the *C. elegans* embryo in a single layer of epidermal cells. This process is initiated by the migration and adhesion of two pairs of anterior leading cells, followed by the migration and adhesion of eight pairs of posterior pocket cells. The migration of the leading cells is mediated by F-actin rich filopodia-like protrusions, which are under the control of the Rac – Wave/Scar – Arp2/3 pathway. Cables of F-actin become enriched around the margins of the pocket cells to form a ring, and early studies showed that this ring is under tension. Based on this data, actomyosin contractility was predicted to mediate the closure of this ring during ventral enclosure. However, nonmuscle myosin has not been studied in ventral enclosure, where it could regulate ring closure in addition to regulating cell shape changes and/or adhesion. For example, proteins that form adhesion junction complexes are also required for ventral enclosure, as they maintain contacts between cells so they can migrate as a unit and form new junctions with contralateral neighbors.

Our studies support a role for myosin contractility in ventral enclosure. RhoA regulates nonmuscle myosin contractility for cytokinesis in the early embryo and for elongation of the lateral epidermal cells in late embryogenesis. ECT-2 is the GEF that activates RhoA during cytokinesis, and a different GEF, RHGF-2, activates RhoA during late embryogenesis. A hypomorphic, maternal ts allele of *ect-2*, *ax751*, is required for polarity in the early embryo, but displays few cytokinesis defects, especially at non-permissive temperatures. Using this allele, we found that *ect-2* is required for the migration of neuroblasts during earlier embryonic stages, and ventral epidermal cells during ventral enclosure. Genetic crosses suggest that *ect-2* functions in parallel to the Rac pathway and may be part of the Rho pathway to regulate actomyosin contractility, supporting a role for myosin in ventral enclosure. Imaging and quantification of embryos expressing GFP-tagged myosin showed that myosin forms into a supracellular structure around the margins of the ventral pocket cells, reminiscent of the actin ring described previously. We found that *ect-2* is required for the enrichment and organization of myosin, supporting a requirement for *ect-2* in regulating myosin contractility. Interestingly, *ect-2* may also function in the cadherin/catenin pathway that forms adhesion junctions, suggesting *ect-2* could also regulate the actomyosin filaments that contribute to adhesion.

Acknowledgments

Gabriel and Melina; only with their help, I can achieve such good quality data for this thesis.

Contributions of Authors

Figure 8: Alvaro Marte (BIOL490 student) contributed by *ect-2(ax751);* AJM-1:GFP filming and measurement of cell migration velocity.

Table 9: Neetha Makil contributed by making *ect-2(zh8);rho-1(ok2418)* mutant, and its phenotype counting.

Figure 11: Karina Mastronardi contributed by DIC filming for *let-502(sb118)*

Table of Contents

List of Figures

List of Tables

x

Chapter 1. Introduction

Organs form during embryonic development by the morphogenesis of cells that undergo coordinated shape changes and migration. Many homeostatic events, such as wound healing, also require cells to coordinate shape changes and migration. Furthermore, similar types of cellular events drive metastasis: the spreading of cancer cells to other parts of the body (Bompard et al., 2005). Therefore, understanding how cells change shape and migrate, particularly in a coordinated manner, can shed light on how morphogenetic events are regulated for various processes including development, wound healing, and cancer (Wong and Schwarzbauer, 2012). Invertebrate models such as *Caenorhabditis elegans* are ideal to use for studying tissue morphogenesis. Due to its rapid life-cycle (3.5 day at 20ºC), transparency, genetics, and amenability to transgenics and RNAi, *C. elegans* are well-suited for light microscopy, and visualization of tissue formation during development (Figure 1) (Glavis-Bloom et al., 2012). Maternally-expressed proteins are loaded into oocytes within the germline and regulate early embryogenesis. Depending on the gene, zygotic expression may start in mid-embryogenesis, and transition to full zygotic requirement by late embryogenesis (Newman-Smith and Rothman, 1998). Epidermal morphogenesis is initiated during mid-embryogenesis by the intercalation of cells on the dorsal side of the embryo, and is followed by the migration of ventral epidermal cells to form a tissue around the embryo (Williams-Masson et al., 1997). The simple organization of this tissue, availability of markers, and the high degree of conservation in the timing and order of events in wild-type embryos makes it
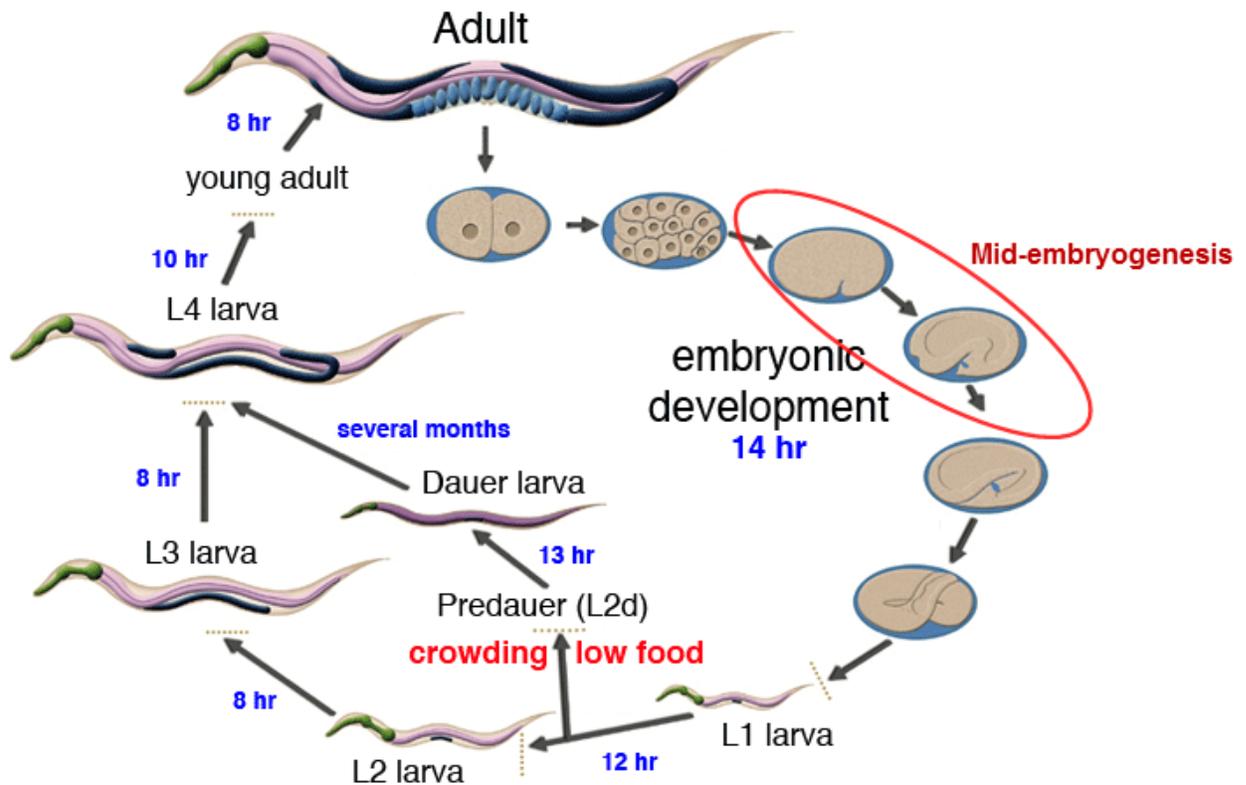
Figure 1. *C. elegans* life cycle. The life cycle of *C. elegans* at 22^0C is shown from the first cell division, through embryonic development, larval development and to adulthood. The stages of embryogenesis that are shown are the first cell division (2-cell stage), gastrulation, and mid-late events including ventral enclosure and elongation. Embryos in mid-embryogenesis are circled, which is when many genes transition from maternal to zygotic expression. When food is low, L1 larva can exit the life cycle and become a dauer form that is highly resistant to changes in temperature, dehydration and limited food supplies. This figure is adapted from artwork by Altun and Hall, Wormatlas (2008).

ideal for studying how the cytoskeleton is regulated to mediate changes in cell shape and migration for morphogenetic events.

1.1 *C. elegans* embryogenesis

1.1.1 Gatrulation: from cell division to tissue specific

C. elegans epidermal morphogenesis occurs through several distinct steps. All epidermal cells are born as six rows of cells on the dorsal surface of the embryo. In the first step of tissue formation, dorsal epidermal cells intercalate on the dorsal surface of the embryo (*dorsal intercalation*), and in the second step, ventral epidermal cells change shape and migrate toward the ventral midline where they adhere (*ventral enclosure*). Subsequently, the epidermal cells constrict to drive the overall shape change of the worm (*elongation*). However, prior to epidermal morphogenesis, there are other migratory events that occur in the early embryo to produce the future tissues of the organism. For example, when embryos reach the 26-cell stage, gastrulation begins by the migration and ingression of cells to form 3 germ layers; endoderm, ectoderm, and mesoderm. Precursor cells for internal organs (*e.g.* intestine, germline, and pharynx) and body wall muscle ingress from the ventral surface of the embryo, leaving a depression, known as the ventral cleft. The ventral cleft is surrounded by neuroblasts, which subsequently migrate to fill in the space by a process known as *ventral cleft closure* (Pohl et al., 2012). The machinery that regulates cell migration and shape changes for gastrulation and ventral cleft closure likely uses some of the same components that regulate epithelial morphogenesis in later development (Chisholm and Hardin, 2005). In support of this, mutations in genes

3

required for the migration of ventral epidermal cells during ventral enclosure are also required for the migration of neuroblasts during ventral cleft closure (George et al., 1998; Chin-Sang et al., 1999; Bernadskaya et al., 2012). Furthermore, actomyosin contractility (see section 1.4) is essential for the constriction of epidermal cells during elongation, and also is required for the ingression of cells during gastrulation (Piekny et al., 2000; Lee and Goldstein, 2003).

1.1.2 *C. elegans* embryogenesis: ventral enclosure and elongation

Ventral enclosure begins with the migration of two pairs of anterior-positioned ventral epidermal cells (*leading cells*) toward the ventral midline, where they meet and form new junctions with their contralateral neighbours (Figure 2) (Williams-Masson et al., 1997; Chisholm and Hardin, 2005). Migration of the leading cells is crucial for ventral enclosure; inactivation of these cells by laser ablation can inhibit ventral enclosure and cause the embryo to rupture during elongation (Williams-Masson et al., 1997). Their migration requires the formation of filopodia, and relies on pathways that regulate the formation of short, branched F-actin (Patel et al., 2008). Posterior-positioned ventral epidermal cells (*ventral pocket cells*), subsequently migrate and adhere with their contralateral neighbours at the ventral midline (Chin-Sang and Chisholm, 2000; Chisholm and Hardin, 2005). These cells do not form filopodia and instead have F-actin cables at their margins, which appear to form a ring. This pattern lead to the prediction that they close via a purse-string like mechanism, which requires actomyosin contractility (Williams-Masson et al., 1997). Once ventral enclosure has
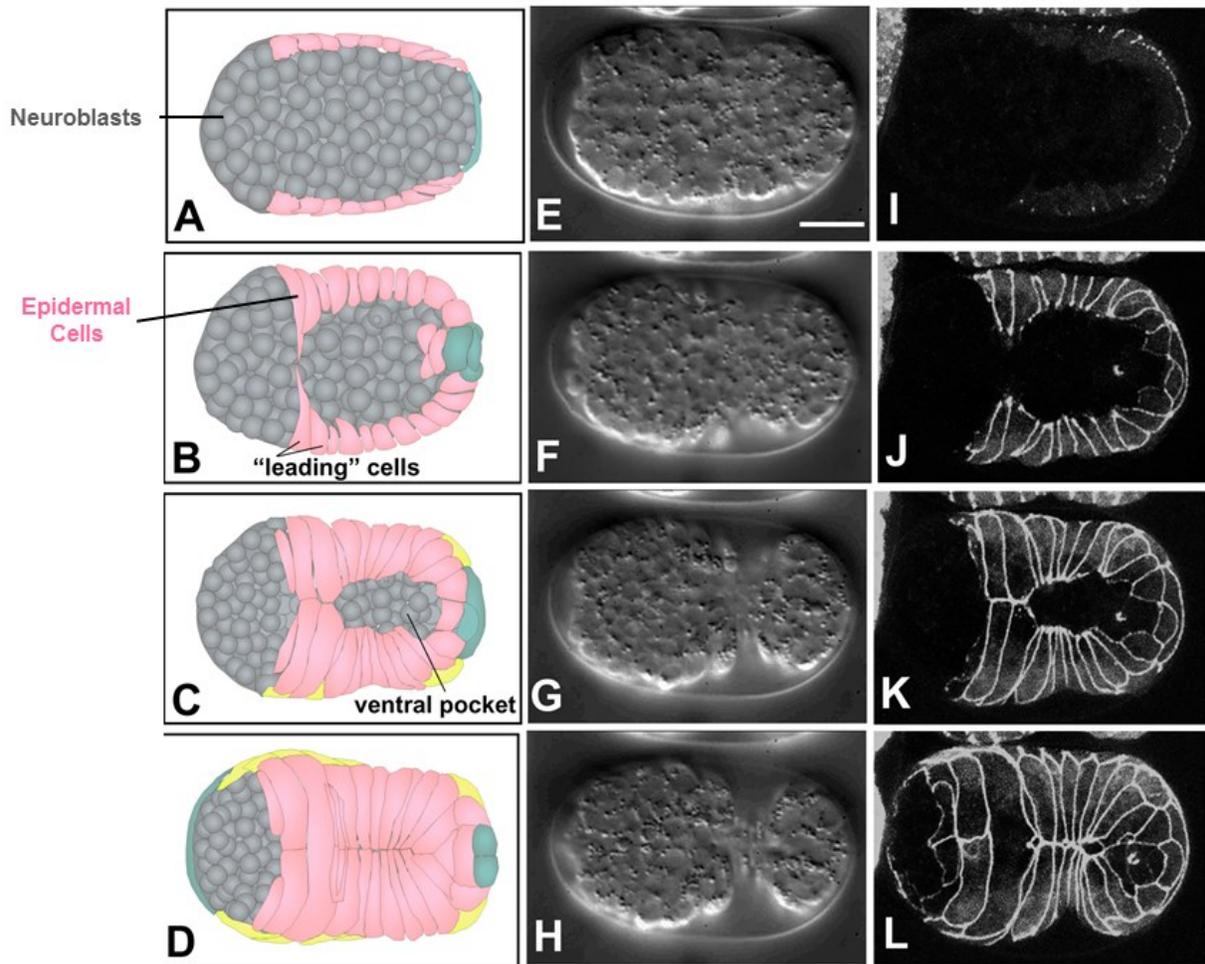
Figure 2. *C.elegans* ventral enclosure. During mid-embryogenesis, (A-D) epidermal cells (pink) initially born in the dorsal side extend, migrate on top of neuroblasts (grey) to adhere at the ventral midline. Starting by migration and adhesion of leading cells, then follow by the closure of ventral pocket cells at the ventral midline. (E-H) Show correspondent DIC image of VE process, and (I-L) show embryo expressing fluorescent marker in epidermal cells undergoing VE. Figures adapted from Chisholm and Hardin (2005).

completed, the embryo is wrapped in a single layer of epidermis and undergoes elongation.

Elongation is driven by the constriction of lateral epidermal cells (*seam cells*), which elongates the embryo along the anterior-posterior axis, and transforms the embryo into the typical long-thin worm shape (Priess and Hirsh, 1986; Chisholm and Hardin, 2005). This process is driven by a combination of actomyosin contractility within the seam cells, which transforms their shape from a cube to a cylinder, and mechanotransduction from the underlying muscle cells (Piekny et al., 2003; Zhang et al., 2011). Mutations in genes that affect contractility, or disrupt the underlying muscle cause elongation phenotypes (Williams and Waterston, 1994; Shelton et al., 1999; Piekny et al., 2000).

1.2 Ventral enclosure regulation

1.2.1 Cell migration

The migration of ventral epidermal cells is essential for ventral enclosure, and is driven by the formation of long, thin actin-enriched protrusions at the leading edge of the cells that extend toward the ventral midline. When epidermal cells meet and adhere with their contralateral neighbors, filamentous actin (F-actin)-rich protrusions overlap and form thick bands of F-actin at the newly forming adhesion junctions (Williams-Masson et al., 1997). Genes required to form the filopodia/lamelipodia protrusions encode GTPase Rac/CED-10, the Wave/Scar complex, and Arp2/3. In this pathway, Rac/CED-10 activates the Wave/Scar complex (comprised of GEX-2, GEX3, ABI-1 and WVE-1), which serves as a nucleation-promoting-factor to activate the Arp2/3 complex for the

6

polymerization of short, branched F-actin (Figure 3) (Soto et al., 2002; Patel et al., 2008; Shakir et al., 2008). Arp2/3 complex can also be activated by members in the WASP protein family, which are homology proteins with Wave/Scar, share conservative domains respond for binding and activating Arp2/3. Unlike Wave/Scar, WASP proteins are auto-inhibited and activated upon Cdc-42 activation (Pollitt and Insall, 2009). Mutations in any of these genes impede cell migration, causing the ventral epidermal cells to remain on the dorsal surface of the embryo and the internal contents of the embryo to extrude, causing the 'Gut on the exterior' (Gex) phenotype (Soto et al., 2002; Sawa et al., 2003; Patel et al., 2008).

In other cell types, nonmuscle contractility provides forces in the rear of the cell for migration, however it is not known if myosin is required for ventral epidermal cell migration. As ventral epidermal cells migrate, they lengthen and undergo apical constrictions, and myosin could be required to mediate these changes. Furthermore, as described earlier, the closure of the pocket cells likely occurs by contractility to close them by a purse-string mechanism. However, it has been challenging to study a role for myosin in ventral enclosure due to the lack of ts (temperature sensitive) alleles in the pathway that regulates myosin contractility. Many of these components are maternally required for cytokinesis in the early embryo, and zygotically required for elongation during late embryogenesis. Therefore, ts alleles are essential for studying requirements in the transition period during mid-embryogenesis.

Rac → WAVE/Scar ⟶
                      ↘
                        Arp2/3→ Branch F-Actin → Migration
                      ↗
Cdc42 → WASP
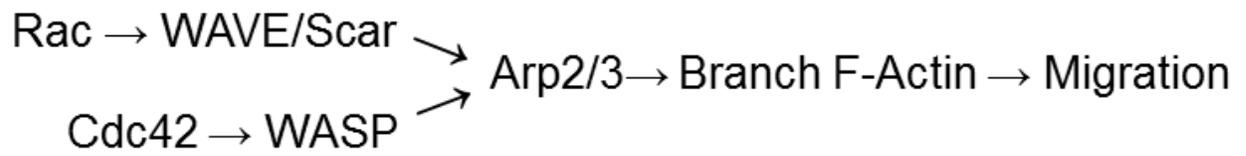
Figure 3. The Rac/Cdc-42 pathway for cell migration. This schematic shows the pathway that is regulated by the small GTPases, Rac and Cdc-42, for cell migration. Upon their activation, Rac or Cdc42 will regulate downstream effectors including WASP or WAVE/Scar to activate Arp2/3 to form branched F-actin. These actin filaments are important for forming lamellipodia or filopodia at the cell front for migration (Pollitt and Insall, 2009).

1.2.2 <u>Adherens junctions</u>

Tissue morphogenesis requires cells to change shape and migrate in a coordinated manner. Adhesion junctions form between neighbouring epithelial cells, which transmit forces across multiple cells and allow them to move as a unit. *C. elegans* epithelial cells contain two adhesion complexes: the cadherin-catenin complex (CCC) and the DLG-1/AJM-1 complex (DAC) (Figure 4) (Labouesse, 2006). The CCC is the most apical complex in the junction, and contains multiple components. E-cadherin (HMR-1) is a transmembrane protein with an extracellular domain that homotypically binds to other E-cadherins, and an intracellular domain that interacts with other proteins. In this way, E-cadherin functions to directly link neighbouring cells (Costa et al., 1998). In addition, α-catenin (HMP-1) binds to F-actin, and β-catenin (HMP-2) crosslinks α-catenin to E-cadherin (Costa et al., 1998; Labouesse, 2006). The DLG-1/AJM-1 complex is more sub-apical in comparison to the CCC, and includes DLG-1 (homologue of Discs large in *Drosophila*), and AJM-1, a coiled-coil protein (Labouesse, 2006). These junctions allow forces to be transmitted across cells, which is important for tissue formation and to maintain tissue integrity (Loveless and Hardin, 2012). Genes that regulate cell adhesion and encode components of the CCC are required for ventral enclosure. Ventral epidermal cells still migrate toward the midline in CCC mutant embryos, but cells fail to form stable contacts with contralateral neighbours and display rupture phenotypes or variable abnormal body morphologies (Costa et al., 1998; Labouesse, 2006). In mammalian cells,
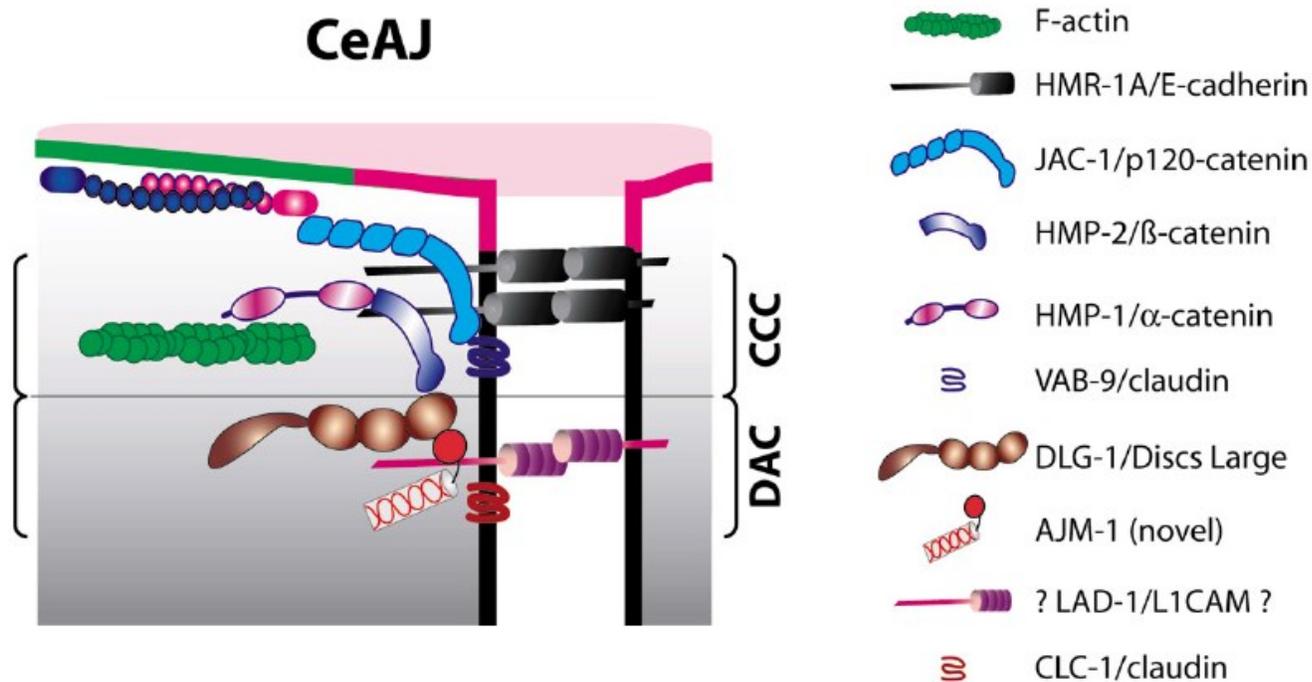
Figure 4. *C. elegans* adherens junctions. This cartoon shows the adherens junction in a *C. elegans* epithelial cell. These junctions are comprised of the cadherin-catenin complex (CCC) and the DLG-1/AJM-1 complex (DAC). The legend on the right shows the different components in the two complexes, which work together to maintain cell-cell adhesion, and allows forces to be transmitted across cells through the intracellular actin cytoskeleton. Cells lacking both CCC and DAC components have rounded epithelial cells that cannot adhere. This figure is adapted from Labouesse (2006).

nonmuscle myosin is required for junction formation and stability, but it is not known if myosin contributes to junctions in *C. elegans* embryos (Vicente-Manzanares et al., 2009).

1.3 Neuroblasts and their role in epidermal morphogenesis

As described earlier, neuroblasts migrate to close the ventral cleft that was left after gastrulation. Their movement produces a surface of neuroblasts on the ventral side of the embryo, which serves as a substrate for the migration of ventral epidermal cells during ventral enclosure (Chisholm and Hardin, 2005). The main pathways that regulate neuroblast migration involve the Eph receptor (VAB-1)/Ephrin, PTP-3/LAR RPTP (Leukocyte Common Antigen Related Receptor Protein phosphatase) and semaphorin-2A/MAB-20, known for their roles in axon guidance (Chin-Sang et al., 1999; Chin-Sang et al., 2002; Harrington et al., 2002). Defects in these genes prevent neuroblasts from sorting to their appropriate regions, and result in an enlarged or persistent ventral cleft and abnormal ventral enclosure. The receptors for these pathways (*e.g.* ephrin and semaphorin) are also expressed in the epidermal cells, and the cues secreted from the neuroblasts signal these receptors to help guide the migration of ventral epidermal cells toward the ventral midline (Bernadskaya et al., 2012).

There are still a lot of open questions about the role of neuroblasts in mediating ventral epidermal cell migration, particularly since the receptors for secretory cues are found in both the neuroblasts and in the overlying epidermal cells. Tissue-specific rescue experiments suggest that ventral epidermal cell migration only requires the expression of receptors in the epidermal cells

11

(Ikegami et al., 2012). However, the source of the cue is not well understood, and there are several pathways involved in ventral enclosure, and their relative contributions are not well understood. Furthermore, neuroblast division and position is essential for ventral enclosure, but it is not clear if this is because the cue no longer forms the appropriate gradient, or if there are mechanical functions provided by the neuroblasts (Fotopoulos et al., 2013). For example, one subset of ventral neuroblasts serve as a 'bridge' for the migration of overlying ventral epidermal cells, and changes in their position or shape lead to the misalignment and failure of ventral pocket closure during ventral enclosure (Ikegami et al., 2012).

1.4 <u>Molecular regulation of actomyosin contractility</u>

1.4.1 <u>F-actin</u>

While formins are not known to be required for ventral enclosure, the formation of F-actin bundles at the apical ends of epidermal cells during closure of the ventral pocket supports their requirement. Actomyosin contractility uses F-actin that is long and unbranched, which is polymerized by formins. Formins contain several domains that are required for their regulation and function. At the core of the protein are the FH1 and FH2 domains: the FH1 domain binds to profilin-bound actin monomers, while the FH2 domains homodimerize to form a donut structure (Xu et al., 2004). This donut associates with the barbed end of the growing F-actin filament, and the FH1 domains extend out, bind to profilin-actin monomers and assemble them into the filament (Pruyne et al., 2002). Formins also contain a DID and a DAD domain, which interact and inhibit formin

activity by preventing dimerization of the FH2 domains. Active RhoGTPase binds to a domain that overlaps with the DID to relieve this autoinhibition (Goode and Eck, 2007). Formin-polymerized F-actin is crucial for actomyosin contractile events such as cytokinesis, cell shape changes during epithelial morphogenesis, and formation of stress fibers during migration (Pollard, 2007).

1.4.2 **Myosin**

While myosin is not known to be required for ventral enclosure, one of the persisting models used to describe closure of the ventral pocket relies on actomyosin contractility. This model was derived from the observation that a ring of bundled F-actin forms around the pocket cells, which appears to constrict as they close (Williams-Masson et al., 1997). Purse-string mechanisms have been described for other cellular events including wound healing, where an actomyosin cable forms along the wound edge and constricts to close the wound, and cytokinesis, where an actomyosin ring pinches in the cell to form two daughter cells (Bement et al., 1993; Piekny et al., 2005). Nonmuscle myosin is also required for apical constriction, which changes cell shape for morphogenetic events such as dorsal closure in *Drosophila* and gastrulation in *C. elegans* (Franke et al., 2005; Roh-Johnson et al., 2012).

In nonmuscle cells, nonmuscle myosin II is the main myosin that cross-links actin filaments and produces contractile forces. Myosin is a hexamer with two pairs of heavy chains (NMY-1 or NMY-2 in *C. elegans*), two pairs of essential light chains (MLC-3 in *C. elegans*) and two pairs of regulatory light chains (RLC; MLC-4 in *C. elegans*). Myosin activity is regulated by phosphorylation of the RLC,

which promotes dimerization of the heavy chains and stimulates ATPase activity in the motor domain (Vicente-Manzanares et al., 2009). Several kinases phosphorylate RLC, including Rho-associated kinase (ROK) and citron kinase, both of which are Rho effectors that are regulated by binding to active RhoA (Matsumura, 2005). The activity of myosin is also negatively regulated by myosin phosphatase, which removes the phosphate from RLC (Matsumura and Hartshorne, 2008). Interestingly, ROK can also phosphorylate and inhibit the regulatory subunit of myosin phosphatase to promote myosin activity (Vicente-Manzanares et al., 2009).

In *C. elegans*, non-muscle myosin and its regulators (e.g. *mlc-4, let-502* and *mel-11*) are required for multiple actomyosin contractile events throughout embryogenesis, including cytokinesis, gastrulation and elongation (Shelton et al., 1999; Piekny et al., 2000; Piekny and Mains, 2002; Pohl et al., 2012). However, due to the limitations of existing alleles and effects of RNAi, which causes defects in early embryogenesis, studies have not yet investigated requirements for myosin contractility during ventral enclosure.

1.4.3 <u>The RhoGEF ECT-2</u>

In mammalian cells, Ect2 was initially identified as oncogene due to its ability to transform cells (Miki et al., 1993). Overexpression or un-regulated Ect2 can cause abnormal cell morphologies and tumor formation in mice (Takai et al., 1995). Ect2 has two BRCT domains in its N-terminus, which form a phosphor-binding motif, and autoregulates Ect2 activity. This domain mediates the formation of an inactive conformation of Ect2 that is relieved when Ect2 binds to

other proteins. The C-terminal half of Ect2 contains lipid binding motifs and a GEF domain, which catalyzes the exchange of GDP to GTP on RhoGTPases (Morita et al., 2005). One of Ect2's best-described functions is for cytokinesis. It generates active RhoA, which binds to effectors such as formins for the polymerization of F-actin, as well as ROK and citron kinase to facilitate RLC phosphorylation for myosin activation. This leads to the formation and ingression of an actomyosin ring to pinch the cell into two daughter cells (Piekny et al., 2005). In cancer cells, Ect2 is no longer sequestered to the nucleus in interphase, and is retained in the cytoplasm where it activates RhoGTPases for tumor cell growth, invasion and migration (Fields and Justilien, 2010). For example, in brain cancer cells (glioblastoma), Ect2 activates Cdc42 and Rac for their migration and invasion (Kwiatkowska et al., 2012).

ECT-2 and other components of the RhoA pathway are conserved in *C. elegans* where they regulate cytokinesis in the early embryo (Figure 5) (Shelton et al., 1999; Piekny and Mains, 2002; Severson and Bowerman, 2002; Dechant and Glotzer, 2003). Therefore, it is difficult to study the requirement for myosin contractility in later stages of embryonic development. Using zygotic-specific alleles, these components were shown to be required during late embryogenesis, to mediate cell shape changes for elongation (Shelton et al., 1999; Piekny et al., 2000; Piekny et al., 2003). However, ECT-2 does not function at this stage of development, and instead a different RhoGEF, RHGF-2, activates RhoA to regulate myosin contractility for elongation (Lin et al., 2012). *C. elegans ect-2* has additional functions that are not related to its role in cytokinesis. In early *C.*
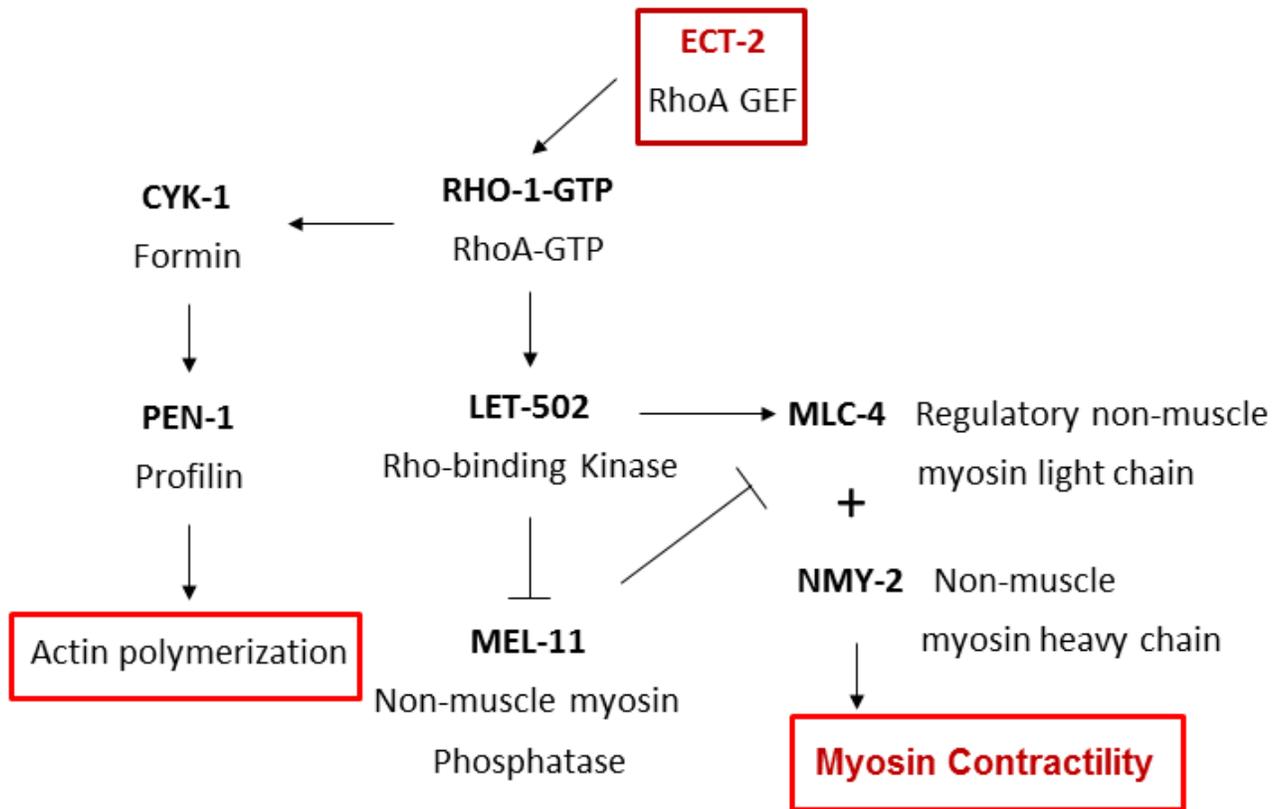
Figure 5. Actomyosin contractility pathway in the early embryo. This schematic shows the pathway that regulates actin polymerization and nonmuscle myosin contractility during early embryogenesis. ECT-2 is a Rho GEF that activates RHO-1, which binds to effectors for actin polymerization (formins and profilins) and nonmuscle myosin contractility (Rho-binding kinase). Myosin is comprised of the regulatory light chain (MLC-4) and heavy chain (NMY-2), and its activity is regulated by phosphorylation of MLC-4. Myosin phosphatase (the regulatory subunit is MEL-11) counteracts Rho-binding kinase and dephosphorylates myosin light chain.

16

elegans embryos, *ect-2* is also required for anterior-posterior polarity, and this function occurs via its regulation of RhoA (Zonies et al., 2010). Also, depletion of zygotic *ect-2* causes adult sterility, which arises due to defects in the division and migration of epidermal P cells, a subset of vulva precursor cells (Morita et al., 2005).

1.5   *Drosophila* epidermal morphogenesis as a model for *C. elegans*

In *Drosophila*, Pebble (Pbl) is the ortholog of *C. elegans* ECT-2, and is essential for cytokinesis and migration (Smallhorn et al., 2004). Pbl activates Rho1 at the cell cortex to orchestrate the formation and ingression of the actomyosin contractile ring for cytokinesis. During gastrulation, Pbl regulates myosin contractility for the apical constriction and internalization of precursor mesodermal cells. Interestingly, the apically-enriched actomyosin fibres are linked by junctions to form a supracellular meshwork, which provides forces that drive the internalization of mesoderm precursors (Martin et al., 2010). During gastrulation, a subset of epithelial cells undergoes epithelial-mesenchymal transitions (EMT), where their identity is transformed to a mesodermal fate (Lim and Thiery, 2012). The spreading of these mesodermal cells over the ectoderm is Pbl-dependent. This process is largely driven by F-actin rich protrusions, and is regulated by a Pbl-Rac pathway (van Impel et al., 2009). Interestingly, Rho1 and myosin contractility do not seem to be required for mesodermal spreading, although these pathways were determined by genetic suppression, and the

requirement for Rho1 and myosin in other processes may preclude studying their specific roles in migration.

One of the steps in *Drosophila* epithelial morphogenesis is when dorsal epithelial cells cover the dorsal surface of the embryo by a myosin-dependent process called dorsal closure. A second tissue, the amnioserosa (an extra-embryonic structure), acts as a substrate to coordinate the movement of the overlying epidermal sheets to the dorsal midline (Jacinto et al., 2002). Dorsal closure requires cell shape changes, as well as the extension and migration of epidermal cells toward dorsal midline, and contractions from underlying amnioserosa (Kiehart et al., 2000). Importantly, a thick actomyosin cable forms around the edge of the migrating epithelial cells during dorsal closure, and may close epithelial sheets together by a purse-string mechanism, similar to wound healing (Martin and Lewis, 1992; Bement et al., 1993). Actin becomes more intense at the front part of the migrating epidermal cells, which change in appearance from 'scalloped' to a smooth arch, as cells progress (Kiehart et al., 2000). Consistent with a requirement for actomyosin contractility in mediating dorsal closure, null myosin mutants fail dorsal closure, and have lower tension at the edge of the epidermal cells. Mutants for *rho1* have reduced actomyosin cables, and display reduced tension at the front edge of the cells (Lu and Settleman, 1999; Jacinto et al., 2002). Pbl, the *Drosophila* ortholog of ECT-2, is also required for dorsal closure and regulates tension at the front of the migrating epidermal cells (Jankovics et al., 2011). In addition, Rho1 accumulates apically to regulate the formation and stability of adherens junctions during dorsal closure

(Magie et al., 2002). The underlying amnioserosa works as substrate for epidermal cells during dorsal closure, and cells in this tissue display extensive contractions and cell shape changes. Large-scale actomyosin structures assemble at the apical surface to mediate their constriction, which decreases the surface area of amnioserosa. This somehow coordinates the overlying epidermal cells during dorsal closure, and facilitates its disappearance (Kiehart et al., 2000).

1.6 <u>Summary</u>

This thesis describes a role for *ect-2* in *C. elegans* ventral enclosure, an event that occurs during embryogenesis to cover the embryo in epidermal tissue. Our results show that *ect-2* likely functions via *rho-1* (RhoA) to regulate actomyosin contractility, which mediates the migration of ventral epidermal cells. While the precise role of *ect-2* in their migration is not clear, it likely regulates the formation and contractility of an actomyosin supracellular structure that forms around the ventral pocket cells and closes via a purse-string mechanism. In addition, we found that *ect-2* could be part of a genetic pathway that regulates adhesion junctions. These results shed light on conserved mechanisms for regulating tissue formation during embryogenesis.

Chapter 2. Materials and methods

2.1 Strains and alleles

C. elegans stocks were maintained on NGM plates (1.7% w/v agar, 5 mM NaCl, 0.25% w/v Bactopeptone, 1 mM $CaCl_2$, 5 µg/mL cholesterol, 25 mM KH_2PO_4, and 1 mM $MgSO_4$) and fed with *E. coli* (OP-50) cultured in LB media (1% w/v tryptone, 0.5% w/v yeast extract, and 170 mM NaCl) according to standard protocol (Brenner, 1974). The following strains were obtained from the *Caenorhabditis* Genetics Center (CGC): N2 (wild-type*), ect-2(ax751) II*, *wsp-1(gm324) IV, ced-10(n3246) IV, ced-10(n1993)*IV, *mlc-4(or253)/qC1 dpy-19(e1259) glp-1 (q339)* III, *unc-119(ed3)* III; tjls1[*pie-1*::GFP::*rho*-1+unc-*119*(+)], *ajm-1(ok160)* X; jcEx44, *rho-1 (ok2418)/nT1 [qls51])*, *rde-1 (e219)*, and *hmp-2(qm39) I*. The following strains were obtained from colleagues: *let-502(sb118)* from P. Mains (University of Calgary), *unc-4(e120); ect-2(zh8) II* from A. Hajnal (University of Zurich), *ect-2(gk44) II; unc-119(ed3) III; xnls162 [ect-2::GFP + unc-119(+)]* from J. Nance (Skirball Institute), and *nmy-2(cp7[nmy-2::gfp + LoxP unc-119(+) LoxP]) I* from B. Goldstein (University of North Carolina). The following strains were made for this thesis: *ect-2(ax751);* AJM-1:GFP, *ect-2(ax751)*; *wsp-1(gm324), ect-2(ax751)*; *ced-10(n3246), ect-2(ax751)*; *ced-10(n1993), ect-2(ax751)*; *rho-1 (ok2418)/+, ect-2(ax751)*; *mlc-4 (or253)/+, ect-2(ax751) II*; *let-502(sb118)*, NMY-2:GFP; *ect-2(ax751),* NMY-2:GFP; *ect-2(zh8),* and *ect-2(zh8) II; rho-1 (ok2418)/+*. All strains maintained at 15°C except GFP fluorescent expression strains at 20°C.

2.2 <u>Genetic crosses</u>

Genetic crosses were performed to determine functional requirements for *ect-2*. L4/young adult hermaphrodites and L4/young adult male worms were placed on NGM plates seeded with *E. coli* in small circles in the centre of the plate (e.g. 2-3 cm diameter) to maximize their interactions. Broods were scored from F1 (to assess maternal requirement of *ect-2*), F2 (to assess genetic interactions for double mutant combinations using zygotic alleles) or F3 progeny (to assess genetic interactions for double mutant combinations using maternal alleles) using standard protocols and Chi-square analyses were performed to assess genetic interactions (Mains et al., 1990). One modification we adopted was to use eight or more L4 stage hermaphrodites, each brooded on two plates with a minimum of 30 eggs per plate. For crosses using temperature sensitive strains, such as *ect-2(ax751)* and *let-502(sb118)*, crosses were performed at 20°C, and the L1's (*let-502* - zygotic) or L2's (*ect-2* - maternal) were upshifted as L4 stage hermaphrodites to 25°C to access lethality of the F2 or F3 generation at restrictive temperature. Phenotypes were determined as indicated in the figures and tables.

2.3 <u>Immunostaining</u>

ECT-2:GFP embryos were fixed and immunostained for GFP in order to reveal the expression pattern of ECT-2. First, gravid hermaphrodites were treated with a bleach solution (8% bleach and 0.8 M NaOH) to release embryos. Then, the embryos were washed three times using equal volumes of M9 solution

(3.4 mM Na_2HPO_4, 2.2 mM KH_2PO_4, 0.9 mM NaCl, and 0.9 mM NH_4Cl). Embryos were pipetted onto a poly-lysine coated slide. Next, the embryos were freeze-cracked by placing coverslips at an angle on the slide (over the embryos) and placing the slides in liquid nitrogen for a few seconds, or on dry ice for ~30 sec – 1 min, then 'popping' the coverslips off of the slides. A pap pen was used to draw a circle around a central area that had the most embryos. The slides were placed in -20°C methanol for 15 minutes, then washed three times for 10 minutes each with 0.1% TBST (150 mM NaCl, 50 mM Tris HCl pH 7.6 and 0.1% Tween-20). For all of the immunostaining steps, the slides were placed in 'chambers', made using covered plastic dishes with parafilm and wet paper towels. After washing, the embryos were blocked by adding 5% NDS in 0.1% TBST for 30 min at room temperature. Then, they were incubated with 1:100 dilution of rabbit anti-GFP polyclonal antibodies (gift from Michael Glotzer's lab, University of Chicago) and 1:10 mouse MH27 monoclonal antibodies (anti-AJM-1; Developmental Studies Hybridoma Bank) in 5% NDS in 0.1% TBST for two hours at room temperature. After washing three times with 0.1% TBST, the slides were incubated with secondary antibodies (1:250 anti-rabbit antibodies coupled with 488 and1:250 anti-mouse antibodies coupled with 568; Invitrogen) in 0.1% TBST for two hours at room temperature. The slides were then washed three times, and incubated for five minutes with 1:1000 DAPI (1 mg/mL; Sigma) in 0.1% TBST, washed once with 0.1% TBST, then washed with 0.1M Tris HCl pH 8.8, after which a drop of pre-warmed mounting media (5% n-propyl gallate, 50% glycerol, 50 mM Tris pH 9) was added to each slide and coverslips were added and sealed. Similar

22

procedures were followed to visualize RHO-1 and AJM-1 in GFP:RHO-1 embryos.

2.4 <u>Microscopy</u>

We performed live imaging using DIC or fluorescence microscopy to visualize the *ect-2* mutant (single or double) phenotypes. Embryos were collected using established protocols (Sulston et al., 1983). Gravid (egg-carrying) hermaphrodites were transferred to a drop of M9 solution on a depression slide, and dissected by a surgical blade to release the embryos. Embryos were then added to freshly made 2% agarose pads on slides, using a Pasteur pipette bulb coupled to a capillary. Embryos were grouped together using an eyelash glued to a toothpick, to form clusters (permits imaging more embryos at once, but it is important to have less than 8 embryos clustered to avoid oxygen deprivation). Then, coverslips were added to the slides with additional drops of M9 to prevent the slides from drying out during imaging, and coverslips were sealed with prewarmed liquid Vaseline or VALAP. To observe phenotypes during epidermal morphogenesis by Nomarski (DIC), embryos were imaged on the LEICA DMI6000B microscope using the 40X objective, and images were captured every 10 min using a Hamamatsu Orca R2 camera, Piezo Z/ASI stage (MadCityLab), and Volocity acquisition software (PerkinElmer). For optimal movies, we captured 4 Z-planes of 2 μm thickness, every 10 minutes for a total of 7 hours. *ect-2(ax751)*; AJM-1:GFP and control AJM-1:GFP embryos were imaged with the same microscope, but using GFP fluorescence. Time-lapse images were acquired with the GFP filter (Semrock), every 12 min using 8 Z-planes of 1 μm

thickness from the top to medial planes of the embryo. To prevent embryonic lethality caused by phototoxicity, the aperture was closed to 17% to limit light intensity, and exposure times were kept below 300 ms. The gain was increased to offset the low exposure times, but we kept it below 100 to obtain optimal images. To image fixed embryos, images were collected using the same microscope, but using the 63X objective, and collecting Z-planes of 0.3 μm thickness. Alternatively, the Leica TCS SP2 confocal microscope was used to collect images using the 63X objective and Leica confocal software (v1.4), with 500 ms of exposure, 250 gain, and averaging of two. Images of strains expressing AJM-1:GFP, NMY-2:GFP, and ECT-2:GFP were collected using the 60X objective on an inverted Nikon Eclipse Ti microscope outfitted with the Livescan Sweptfield scanner (Nikon), Piezo Z stage (Prior) and the Andor Ixon 897 camera, with Elements 4.0 acquisition software (Nikon) and the 488 laser (set between 10-25% power). Z-stacks of 0.5 μm, for a total distance of 12 μm from surface to the middle of embryo, were collected every 10 min. The gain was kept below 250, and exposure times were below 300 ms. All imaging was performed at room temperature, except a chamber (IBIDI) was used to fix the temperature at 25°C on the Leica DMI6000B microscope when imaging single and double mutant temperature sensitive allelic combinations.

Images were exported into TIFF format to use for post-analysis. Some image sets were deconvoluted with AutoQuant 3.1 (Media Cybernetics), while other sets were processed with ImageJ (NIH Image) to create Z-stack projections, perform image rotation and to crop desired regions. Finally, all images were

converted to 8-bit format, then copied and pasted into Illustrator (Adobe) to make figures or to generate Quicktime (Apple) movies.

2.5 Analysis of cell migration and fluorescent intensity

Measurements of ventral epidermal cell velocities and myosin intensity were performed using Image J. To measure epidermal cell velocity, images expressing AJM-1:GFP were used to visualize the boundaries of the epidermal cells. Z-stack projections of each time point were generated. Then, using the 'line tool' function in Image J, the distance from the 'start' (using images at earlier time points) to the 'end' (using images at later time points) of their movement was determined in pixels for each ventral epidermal cell pair. Based on the objective properties, distance was converted from pixels to µm, and the total distance was divided by the total time to give the velocity in µm per min. The velocities for each cell pair were averaged together, and collected for mutant and control embryos. Standard deviations were calculated, and data was graphed in Excel (Microsoft).

To measure changes in myosin intensity, the 'free hand' selection tool in Image J was used to trace regions enriched with NMY-2:GFP signal along the margins of the migrating epidermal cells over different time points. After selecting the region to be measured, 'ROI manager' was used (under the 'analyze' section) to measure the average intensity and area in pixels. We also measured an ROI in other regions of the embryo to create a ratio of 'relative' pixel intensity in the myosin-enriched regions, vs. other locations in the embryo. This helped control for variations in signal intensity due to bleaching, or other slight changes in

imaging conditions. The intensity ratios were determined for multiple time points

during ventral enclosure and compared between the mutant and control

embryos. Ratios were collected for multiple embryos and averaged together. The

standard deviations were calculated, and data was graphed using Excel

(Microsoft).

Chapter 3. Results

3.1 *ect-2* is maternally required for *C. elegans* embryogenesis

The RhoGEF ECT-2 regulates RHO-1 activity to mediate actomyosin

contractility for cytokinesis in the early embryo, but it is not known if *ect-2*

regulates other events during embryogenesis (Dechant and Glotzer, 2003). In *C.*

elegans larva, *ect-2* regulates epidermal P-cell cytokinesis and migration for

vulva formation, suggesting that it may regulate actomyosin for events other than

cytokinesis (Morita et al., 2005). To study *ect-2*'s functions in later stages of

embryogenesis, we used *ax751*, a temperature-sensitive (*ts*) hypomorphic allele

of *ect-2* that shows few cytokinesis defects at permissive temperatures (Zonies et

al., 2010). First, we determined the lethality of this allele at various temperatures

and used DIC imaging to assess phenotypes (Table 1; Figure 6). At permissive

temperature, *ect-2(ax751)* displayed moderate lethality, 32% (n = 300), and a

spectrum of phenotypes across embryogenesis (Table 1). In *ect-2(ax751)* mutant

embryos, 16% arrest before the onset of ventral enclosure (Table 1). Another

37% mutant embryos failed to complete ventral enclosure, and ruptured with their

internal contents extruding outside of the embryo (Table 1; Figure 6). This

phenotype is called Gex (gut on the exterior), and was first described in

Rac/WAVE pathway mutant embryos (Soto et al., 2002). An additional 5% of the

embryos displayed Vab (variable abnormal body morphology) phenotypes (Table

1; Figure 6). Vab phenotypes are typically seen in embryos mutant for adhesion

junction components, where forces that mediate epidermal morphogenesis are

unevenly distributed across the malformed junctions (Simske et al., 2003). Lastly,

Table 1 *ect-2* is maternally required for ventral enclosure.

Genotype	Temperature (ºC)	Embryonic Lethality%*	DIC Phenotype Analyses**			
			Early%	VE rupture%	Vab%	VE delay%
N2	20	0	0	0	0	0
	25	0	--	--	--	--
ect-2(ax751)	20	32	16	37	5	15
	25	95	42	58	0	0
ect-2(ax751) X N2 males	20	23	--	--	--	--
	25	89	--	--	--	--
ect-2(zh8)	20	31	8	22	0	0
ect-2 RNAi 24hrs	20	100	100	0	0	0

* The sample size for this column was 130 < n < 300; *ect-2(ax751)* is the loss-of-function ts allele, and *ect-2(zh8)* is the gain-of-function allele.

**DIC imaging was performed at room temperature (20-23ºC) for rows indicated as 20ºC, and a chamber was used to hold the temperature at 25ºC for rows indicated as 25ºC; 10 < n < 37. Data that was not determined is represented by '--'.
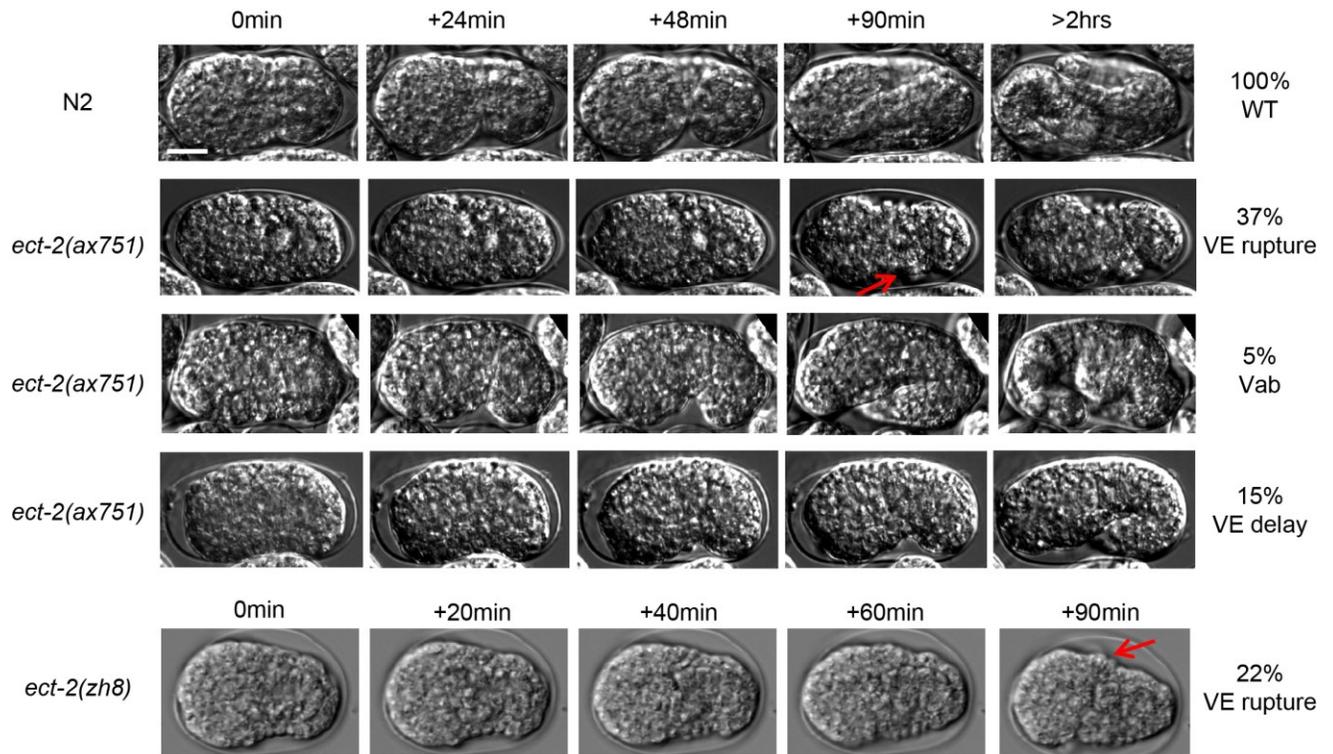
Figure 6. *ect-2* is required for ventral enclosure. At the top are DIC time-lapse images of a wild-type (N2) embryo from the onset of ventral enclosure to the three-fold stage of elongation. Underneath are time-lapse images of *ect-2(ax751)* (loss-of-function) embryos showing the ventral enclosure phenotypes, and the proportion of embryos in each category. The red arrow points to the rupture of the embryo, where the internal contents of the embryos extrude. Also shown is an *ect-2(zh8)* (gain-of-function) embryo, which rupture as indicated by the red arrow. All DIC imaging was performed at room temperature, and 10<n<30 embryos were imaged. The scale bar is 10um.

15% of the embryos had delayed ventral enclosure, but embryos continued to develop similar to wild type embryos (Table 1; Figure 6). While ventral enclosure took less than 50 min to complete in wild-type embryos, it took an average of 90 min for *ect-2* mutant embryos. Consistent with the *ts* nature of the *ax751* allele, embryos at restrictive temperature (25°C) had higher embryonic lethality and earlier phenotypes in comparison to embryos at permissive temperature (Table 1). For example, a higher proportion of embryos arrested prior to ventral enclosure, and no Vab phenotypes were seen (Table 1).

We also examined embryonic phenotypes after *ect-2* RNAi treatment, and in other *ect-2* alleles to determine if we could see mid-late embryogenesis phenotypes similar to the *ax751* allele. Consistent with *ect-2*'s requirement for cytokinesis, *ect-2(RNAi)* embryos displayed 100% lethality, and appeared to have cytokinesis defects (Table 1; data not shown) (Dechant and Glotzer, 2003). However, a gain-of-function (gof) allele, *zh8*, which has excess ECT-2 activity, displayed 31% embryonic lethality (n = 156), and the majority of embryos failed ventral enclosure and displayed Gex phenotypes (Table 1; Figure 6) (Canevascini et al., 2005). The ventral enclosure phenotypes visualized with two of the *ect-2* alleles support a requirement for *ect-2* in *C. elegans* ventral enclosure.

We also tested if *ect-2* is required maternally or zygotically. Ventral enclosure occurs during mid-embryogenesis, at the cusp of when many zygotic genes are expressed. However, a null allele of *ect-2*, *gk44*, is sterile, suggesting that *ect-2* is not required zygotically for embryogenesis. Outcrossing *ect-2(ax751)*

hermaphrodites with wild-type N2 males gave rise to heterozygous *ect-2(ax751)/+* progeny with similar lethality to the homozygous embryos described above, suggesting that *ect-2* is maternally required for embryogenesis (Table 1).

3.1.1   *ect-2* is required for neuroblast migration

Many genes that are required for ventral enclosure, particularly for epidermal cell migration or for adhesion, can display defects in other migratory events earlier in embryogenesis (Chin-Sang et al., 1999; Chin-Sang et al., 2002; Harrington et al., 2002). For example, after gastrulation, a cleft appears on the ventral surface of the embryo and neuroblasts migrate to close this cleft by a process called ventral cleft closure (Chisholm and Hardin, 2005). Delays or defects in their migration can lead to mis-positioned neuroblasts, which could cause ventral enclosure defects, because they act as the substrate for ventral epidermal cell migration (Chin-Sang et al., 1999; Chin-Sang et al., 2002). Using DIC time-lapse imaging, I measured the time required for *ect-2(ax751)* mutant embryos to develop from the 6-cell stage to the onset of ventral enclosure in comparison to control embryos. I observed an average of a 28 min delay (*p<0.01*) in *ect-2(ax751)* (n=12) mutant embryos compared to control embryos (n = 10, Figure 7A), consistent with a requirement for *ect-2* in earlier events in embryogenesis.

Since other ventral enclosure genes also regulate ventral cleft closure, I determined if *ect-2* mutant embryos displayed phenotypes in this process. The ventral cleft appeared near the center of the ventral surface of control (N2)
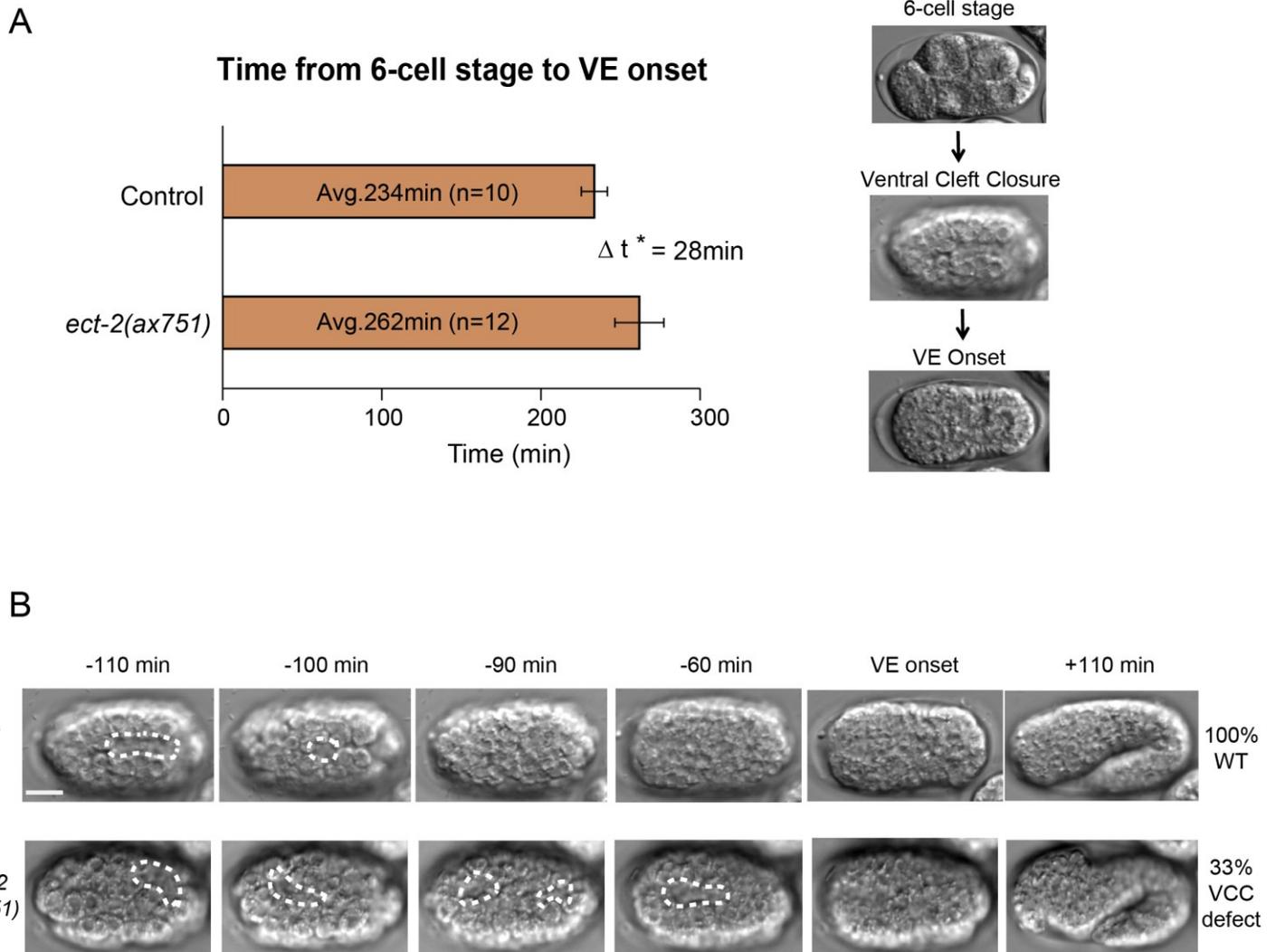
Figure 7. *ect-2* is required for neuroblast migration. (A) The average time for control and *ect-2* mutant embryos to develop from the 6-cell stage to the start of ventral enclosure is shown. *ect-2(ax751)* embryos took 28 min longer to reach VE, *p<0.01 by the student t-test. Bars show standard deviation. DIC images on the right show embryos at the 6-cell stage, ventral cleft closure and onset of ventral enclosure. (B) DIC images show a wild-type embryo going through ventral cleft closure, to ventral enclosure and mid-elongation. Underneath is shown a *ect-2(ax751)* embryo with a mis-positioned and persistent ventral cleft (white dashed line). The percentage of embryos with ventral cleft closure defects is indicated on the right (n = 15 for wild-type and mutant embryos). The scale bar is10 um.

embryos, after which neuroblasts migrated in to close the elongated central cleft in less than 20 min (Figure 7B). However, 33% of *ect-2* mutant embryos displayed persistent or mis-positioned ventral clefts (n = 15, Figure 7B). The ventral cleft appeared in random locations on the ventral surface of the embryo, and persisted for 50 min or longer in some embryos (Figure 7B). Furthermore, all of the *ect-2(ax751)* mutants with visible, persistent ventral cleft closure defects ruptured during later stages of embryogenesis (6/6, Figure 7B). However, not all of the *ect-2* mutant embryos with ventral enclosure defects displayed ventral cleft closure defects, particularly embryos with strong delays. These data suggest *ect-2* is required for multiple events during embryogenesis, including ventral cleft closure, and these earlier requirements could contribute to ventral enclosure phenotypes.

3.1.2 *ect-2* is required for epidermal cell migration during ventral enclosure

Our previous data supports a role for *ect-2* in regulating ventral enclosure. We wanted to further analyze this role to determine 1) if ventral epidermal cells are properly born and positioned prior to ventral enclosure, and 2) if ventral epidermal cells display migratory defects. Particularly since *ect-2* is required for cytokinesis in the early embryo, it was important to know if the ventral enclosure defects in *ect-2* mutant embryos could arise (in part) because there are too few epidermal cells. To address this, I generated an *ect-2(ax751)* strain expressing AJM-1:GFP to mark the epidermal cell boundaries. Using this strain, I performed live imaging at room temperature during mid-embryogenesis, and counted the

number of ventral, lateral (seam cell), and dorsal epidermal cells, and took note of their relative positions. In all of the *ect-2(ax751);* AJM-1:GFP mutant embryos examined, there was no difference in epidermal cell number or position in comparison to control embryos (Table 2). Therefore, the ventral enclosure phenotypes in *ect-2(ax751)* mutant embryos likely are not due to a requirement for maternal *ect-2* in epidermal cell division.

Next, we determined if *ect-2* is required for ventral epidermal cell migration. Together with A. Marte (BIOL 490 student), we performed live imaging with the *ect-2(ax751);* AJM-1:GFP strain to visualize ventral epidermal cell migration. In control AJM-1:GFP embryos, we observed a high degree of conservation in the movement of ventral epidermal cells, similar to what has been previously published (Chisholm and Hardin, 2005). First, two pairs of leading cells migrated in and adhered at the ventral midline, followed by the migration and closure of posterior-positioned pocket cells at the ventral midline. Similar to what I observed using DIC imaging, in control AJM-1:GFP embryos ventral enclosure finished within 50 min (n = 15; Figure 8A). In *ect-2(ax751);* AJM-1:GFP embryos, several ventral epidermal cell migration phenotypes were observed, consistent with what I found using DIC imaging (Figure 8A). One set of mutant embryos displayed migration patterns similar to control embryos, but the ventral epidermal cells took more than twice the amount of time to adhere at the midline (an average of 110 min, n = 10; Figure 8A). In another subset of *ect-2* mutant embryos, the leading cells failed to reach the midline before the ventral pocket attempted to close, and both the

Table 2 *ect-2* **is not required for epidermal cell division.**

Genotype	Ventral Cell*	Dorsal Cell*	Seam Cell*
AJM-1::GFP	11.4	11.9	9.9
ect-2(ax751); AJM-1:GFP	11.3	11.7	9.8

* Imaging was performed at room temperature (>20ºC); n = 8 for each category.
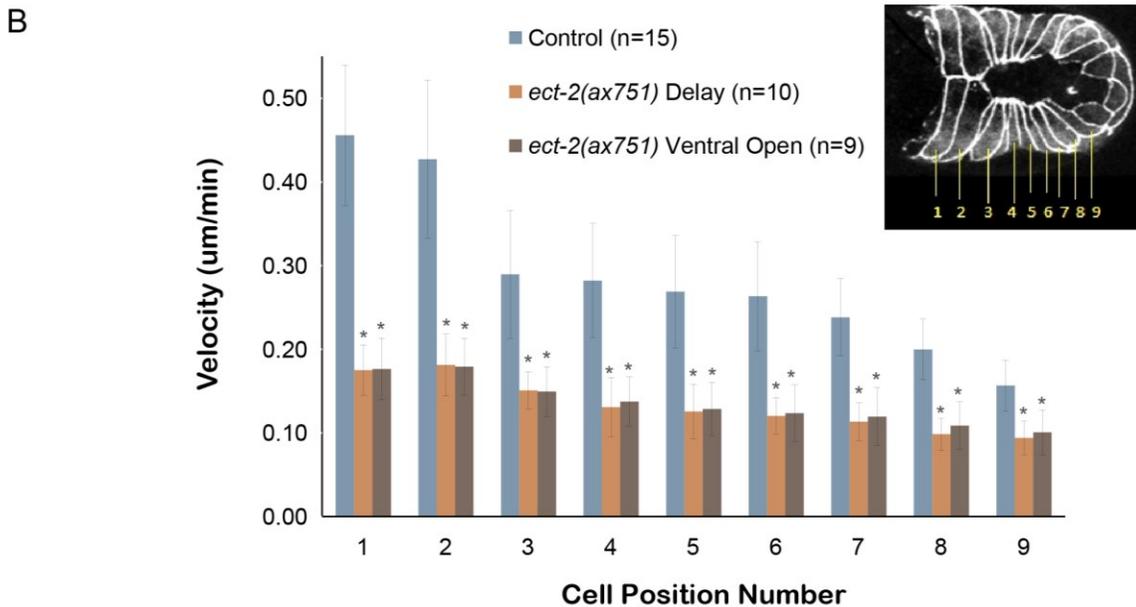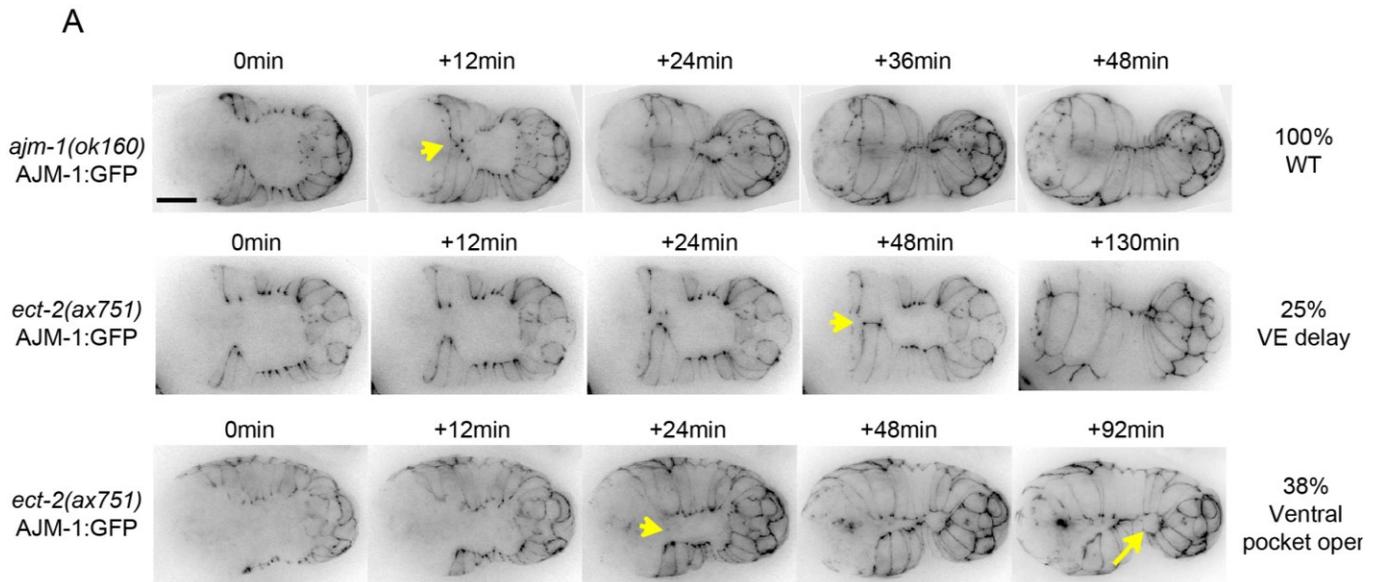
Figure 8. *ect-2* regulates cell migration during ventral enclosure. (A) The top panel shows a control, AJM-1:GFP embryo going through ventral enclosure. Only the ventral epidermal planes are shown, and the cells are clearly outlined. The leading cells are marked by a yellow arrow head, and migrate and adhere at the ventral midline first, followed by the ventral pocket cells. Underneath are shown two different *ect-2(ax751)* embryos with either delay or rupture phenotypes. In both embryos, it takes longer for the VE cells to migrate, and adhere at the midline, or in some, they fail to meet altogether. The percentage of phenotypes is shown on the right. 9<n<15, and the scale bar is 10 um. (B) A bar graph shows the velocity measurements for each ventral epidermal cell pair, as indicated in the embryo above. In control embryos, the first two cell pairs (position 1-2) migrate faster compared to the other cells (position 3-9). In *ect-2(ax751)* mutant embryos, all cells migrate significantly slower compared to control embryos, *$p<0.01$ by the student t-test, regardless of phenotype (blue = control; delay = light orange; ventral open = brown).

leading cells and posterior pocket cells remained open (n = 9; Figure 8A). These embryos displayed rupture as embryogenesis progressed.

Next, we measured ventral epidermal cell velocities in control and *ect-2* mutant embryos (Figure 8B). Each cell pair was numbered from 1 (most anterior pair) to 9 (most posterior pair; Figure 8B). In control embryos, the 2 most anterior leading cell pairs always migrated faster in comparison to the posterior ventral pocket cells (above 0.43 µm/min vs. below 0.29 µm/min; Figure 8B) (Williams-Masson et al., 1997). However, in *ect-2(ax751)* embryos, the velocities of every cell pair were delayed in comparison to control embryos, regardless of the severity of their phenotype (*e.g.* delay vs. failed migration; Figure 8B). In particular, the leading cell pairs were most severely delayed (Figure 8B). For example, while the most anterior leading cell pair (position 1) had a velocity of 0.46 µm/min in control embryos, they only had a velocity of 0.18 µm/min in the *ect-2* mutant embryos. This data suggests that *ect-2* functions to mediate 'robust' migration of the ventral epidermal cells.

3.1.3 <u>ECT-2 is expressed in neuroblasts and epidermal cells</u>

Our data supports a role for *ect-2* in regulating the migration of neuroblasts and ventral epidermal cells. Next, I determined the localization of ECT-2 to determine if it is consistent with its biological requirement. Previous studies showed that ECT-2 is enriched at the anterior cortex in the early zygote, and subsequently localizes around the entire cortex of eight-cell stage embryos (Jenkins et al., 2006; Chan and Nance, 2013). Furthermore, ECT-2 is strongly

expressed in cells required for gonad/vulva formation (Morita et al., 2005).

However, the localization of ECT-2 during mid-embryogenesis was not known.

Recently, Chan and Nance (2013) developed an ECT-2:GFP strain driven by the

ect-2 promoter and showed that this transgene rescued sterility of null *ect-2*

mutant hermaphrodites (*gk44)* (Chan and Nance, 2013). I crossed this transgene

to *ect-2(ax751)* mutant hermaphrodites, to generate a 'rescued' homozygous *ect-2(ax751);* ECT-2:GFP strain that displays no embryonic lethality (Table 3). The

ability of the ECT-2:GFP transgene to rescue the *ect-2(ax751)* phenotypes

suggests that its localization pattern should accurately depict its biological

requirements during mid-embryogenesis. I performed immunostaining with fixed

ECT-2:GFP embryos in ventral enclosure using antibodies to GFP and AJM-1

(MH27; epidermal junction marker). Images showed that ECT-2 is at the

boundaries of epidermal cells (Figure 9). However, ECT-2 appeared to be more

basal in comparison to AJM-1, suggesting that they are in different locations.

ECT-2 was also clearly visible in the neuroblasts underneath the epidermal cells

(within 4 µm) (Figure 9). The localization of ECT-2 to epidermal cell boundaries

supports a role for *ect-2* in directly regulating epidermal cell migration. However,

since ECT-2 is also expressed in neuroblasts, which act as a substrate for the

migrating ventral epidermal cells, *ect-2* could also have a non-autonomous role in

this process.

3.1.4 *rho-1* is required for ventral enclosure

Table 3 ECT-2:GFP transgene rescue of *ect-2* mutants.

Genotype	Phenotype*	GFP Expression
ect-2(gk44)	Sterile	No
ect-2(ax751)	~30% embryonic lethality	No
ect-2(*gk44); ECT-2:GFP and *ect-2(ax751*); ECT-2:GFP	<5% embryonic lethality	Yes

* 90 < n < 200 for each category, except for sterile hermaphrodites.
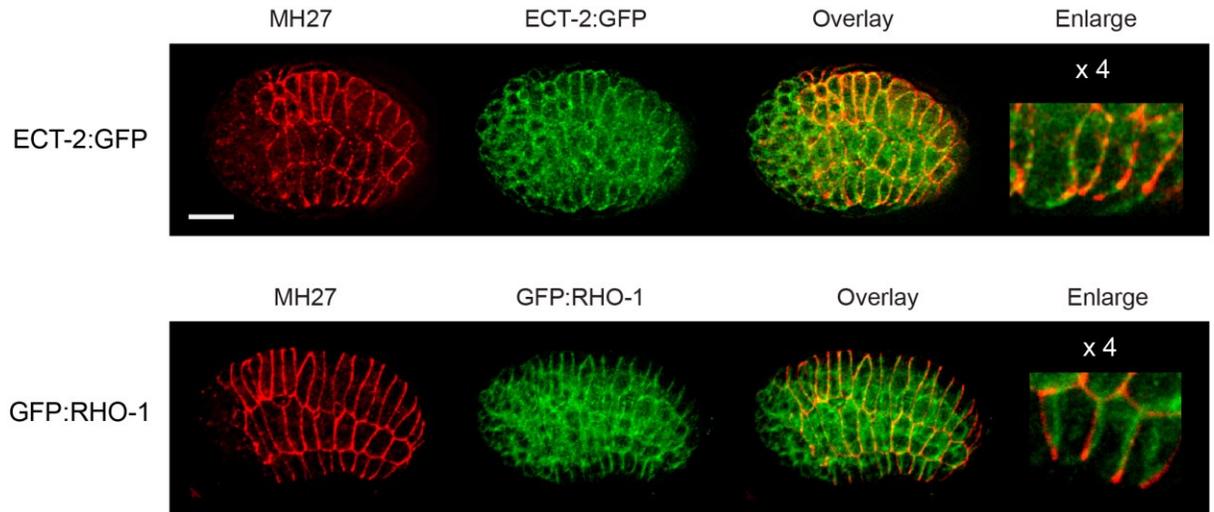
Figure 9. ECT-2 and RHO-1 localize to epidermal cell boundaries and are in neuroblasts during ventral enclosure. ECT-2:GFP (top) or RHO-1:GFP (bottom) embryos were fixed and co-stained for GFP and MH27 (AJM-1 to mark epidermal cell boundaries). In both embryos, GFP had similar expression patterns at epidermal cell boundaries (in a different location from AJM-1) and in the neuroblasts underneath the epidermal cells. The Z planes are 0.3 um and the scale bar is 10 um.

ECT-2 is the RhoGEF that regulates RhoA activity for cytokinesis in the early embryo, and P-cells during larval gonad formation (Dechant and Glotzer, 2003; Morita et al., 2005). However, in other organisms, Ect2 mediates cell migration via regulating Rac activity (van Impel et al., 2009). To determine if *rho-1* is required for ventral enclosure, we examined the localization of RHO-1 and determined its genetic requirement during *C. elegans* mid-embryogenesis. Co-staining GFP:RHO-1 embryos with antibodies to GFP and AJM-1 (MH27), showed that RHO-1 localizes to epidermal cell boundaries and the underlying neuroblasts similar to ECT-2 (Figure 9). RHO-1 also localized more basally in comparison to AJM-1. Genetic assays also revealed a role for *rho-1* in ventral enclosure. We imaged embryos containing a zygotic null allele of *rho-1, ok2418,* which produces a truncated product with no activity (Dvorsky and Ahmadian, 2004). While the majority of homozygous *rho-1(ok2418)* embryos arrested at the 2-fold stage of elongation, a small proportion of the embryos displayed lethality at earlier developmental stages (Fotopoulos et al., 2013). Embryos treated with zygotic-specific *rho-1* RNAi phenocopied embryos carrying the *ok2418* allele, and displayed 59% elongation phenotypes and 41% ventral enclosure phenotypes (n = 38, Figure 10A) (Fotopoulos et al., 2013). Imaging *rho-1(ok2418);* AJM-1:GFP embryos revealed that these earlier phenotypes were consistent with ventral enclosure defects (14%, n = 7). Similar to *ect-2(ax751)* embryos, ventral epidermal cells failed to migrate to the ventral midline, causing the embryos to rupture (Figure 10B). These data support a role for *rho-1* in regulating ventral epidermal cell migration for ventral enclosure, and we propose
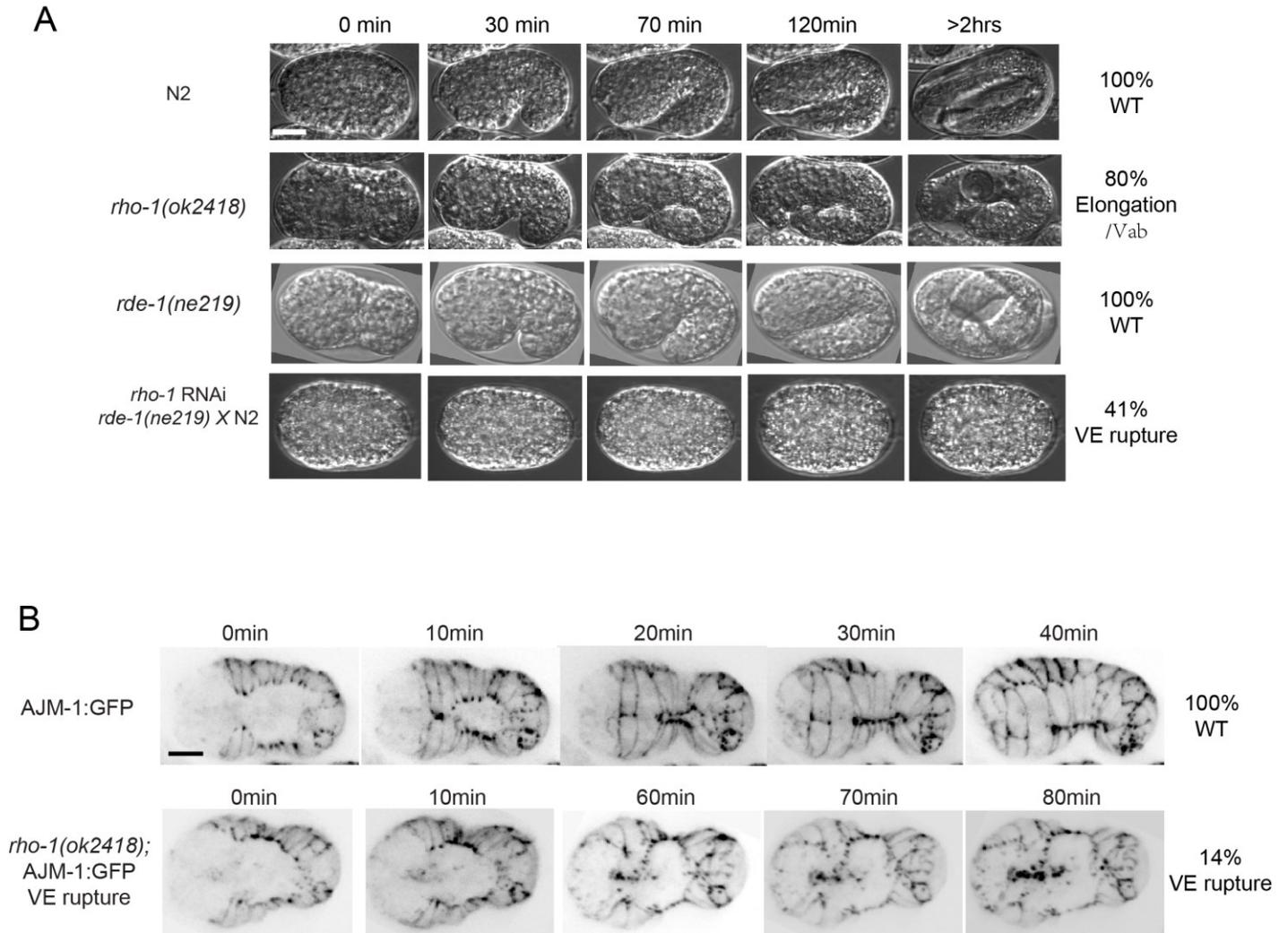
Figure 10. *rho-1* is required for ventral enclosure. (A) The top panel shows DIC images of N2 embryos going through ventral enclosure and elongation. Underneath is a *rho-1 (ok2418)* embryo with an elongation phenotype. Also shown is a control *rde-1* mutant embryo, which displays no embryonic phenotypes and resembles the wild-type embryo. Underneath is shown an *rde-1* mutant embryo treated with *rho-1* RNAi. These embryos had ventral enclosure phenotypes in addition to elongation phenotypes (percentage is shown on the right). (B) Fluorescent images of AJM-1:GFP control and *rho-1 (ok2418);* AJM-1-GFP embryos going through ventral enclosure. The percentage of ventral enclosure rupture phenotypes is shown at the right. The scale bar is 10 um.

that *ect-2* functions in the *rho-1* pathway to mediate ventral epidermal cell migration.

3.2 Determine which genetic pathway *ect-2* functions in during ventral enclosure

3.2.1 *ect-2* likely functions in the Rho pathway

To determine if *ect-2* functions in the *rho-1* pathway to mediate ventral epidermal cell migration, genetic crosses were performed between *ect-2* and components of the Rho pathway, including *rho-1*, *let-502* (Rho-binding kinase), and *mlc-4* (non-myosin regulatory light chain). While the *ect-2* allele is not null, the *rho-1* and *mlc-4* alleles are zygotic null, and the *let-502* allele is ts with strong loss of function phenotypes at restrictive temperature. All of these Rho pathway alleles experience defects in late morphogenesis and produce Vab or elongation-specific phenotypes (grouped as Vab for simplicity) (Shelton et al., 1999; Piekny et al., 2000; Dvorsky and Ahmadian, 2004). If *ect-2* works as a RhoGEF for the Rho pathway, then combining an *ect-2* mutant allele with mutations in the downstream components should not enhance phenotypes. Our data supports this hypothesis, as no or little enhancement of phenotypes was observed between *ect-2* and Rho pathway components (Table 4).

Rather, we found that the total phenotypes were less than additive (weak suppression), supporting that the genes function within the same pathway. We are using hypomorphs or zygotic nulls, and we expect the phenotypes to be additive vs. using maternal nulls where they should stay the same as the

Table 4 *ect-2* may work in the Rho pathway.

Genotype	Temp. (^{0}C)	Vab %	Embryonic Lethality%	Phenotype %*	Expected phenotype%	χ^2 p value	Effect**
N2	20	0	0	0	--	--	--
ect-2(ax751)	20	4.6	27.4	32	--	--	--
	25	0	90	90	--	--	--
ect-2(zh8)	20	0	31	31	--	--	
mlc-4(or253) /qC1	20	23.5	3.6	27.1	--	--	--
let-502(sb118)	20	0	9.2	9.2	--	--	--
	25	87	13	100	--	--	--
rho-1(ok2418)/+	20	18	7	25	--	--	--
ect-2(ax751); mlc-4(or253)/+	20	10.6	47.4	58	59.1	χ^2 =5.38 $p > 0.05$	No effect
ect-2(ax751); let-502(sb118)	20	5	29	34	41.2	χ^2 =10.8 $0.05 < p < 0.01$	Weak Suppression
	25	50	50	100	>100	N/A	N/A
ect-2(ax751); rho-1(ok2418)/+	20	5.5	38.5	45	57	χ^2 =8.25 $0.05 < p < 0.01$	Weak Suppression
ect-2(zh8); rho-1(ok2418)/+	20	4.4	22.2	26.6	56	χ^2 =29.7 $p < 0.01$	Suppression

* Sample size for this column is 100 < n < 400. The percentage of each phenotype were determined as the sum of Vab (Variable abnormal body morphology – hatched as deformed larva) and embryonic lethal phenotypes. Since none of the alleles are maternal null, the expected phenotypes were determined by adding the % of phenotypes for each allele.

** Significance tested by Chi-squared analysis, $0.05 < p < 0.01$ weak effect; $p < 0.01$ strong effect, $p > 0.05$ no effect.

downstream component. However, we observed shifts in the phenotypes depending on the allelic combinations. For example, when combining *ect-2* with *let-502* or *mlc-4*, we noticed an increase in embryonic lethality at the expense of the Vab/elongation-defective phenotypes (Table 4). We also observed an increase in the proportion of early phenotypes (before ventral enclosure) in the *let-502; ect-2* double mutant embryos (Table 5). While we do not know what phenotype caused this early lethality, it could be due to their requirement for cytokinesis or polarity in the early embryo.

Imaging *ect-2(ax751)*; *let-502(sb118)* mutant embryos during mid-late embryogenesis revealed interesting phenotypes where embryos had ventral enclosure phenotypes, but retained epidermal tissue integrity and were less likely to extrude their internal contents (Figure 11, Table 5). The Rho-binding kinase, *let-502*, positively regulates myosin contractility to mediate seam cell shape changes for elongation (Piekny and Mains, 2002; Piekny et al., 2005). We found that the force generated from the elongating seam cells may put pressure of the embryo and cause rupturing when the junctions are not stably formed (Fotopoulos et al., 2013).

We also performed a genetic assay using the gof *ect-2* allele and the zygotic null *rho-1* allele. We predict that since *rho-1* is downstream in the pathway, increasing *ect-2* activity should have no impact on the *rho-1* phenotypes. However, we do not have a maternal allele of *rho-1*, and the allele used in this study is a zygotic null. Since the embryos from heterozygous mothers would have wt maternal *rho-1*, but may have reduced levels vs. wild-

Table 5 *ect-2* ventral enclosure phenotypes are partially suppressed by *let-502*.

Genotype*	Before VE%	VE Rupture%	Vab%	Delay%
N2	0	0	0	0
ect-2(ax751)	16.1	38.7	6.5	16.1
let-502(sb118)	4.3	0	95.7	0
ect-2(ax751); let-502(sb118)	35.3	29.4	35.3	0

* Live imaging performed at room temperature (>20ºC); sample size is 15 < n < 30 per genotype.

|	0 min	20 min	40 min	80min	>2hrs	
Wild Type						100% WT
let-502(sb118)						96% Elongation Arrest/Vab
ect-2(ax751); *let-502(sb118)*						29% VE rupture
ect-2(ax751); *let-502(sb118)*						35% Vab
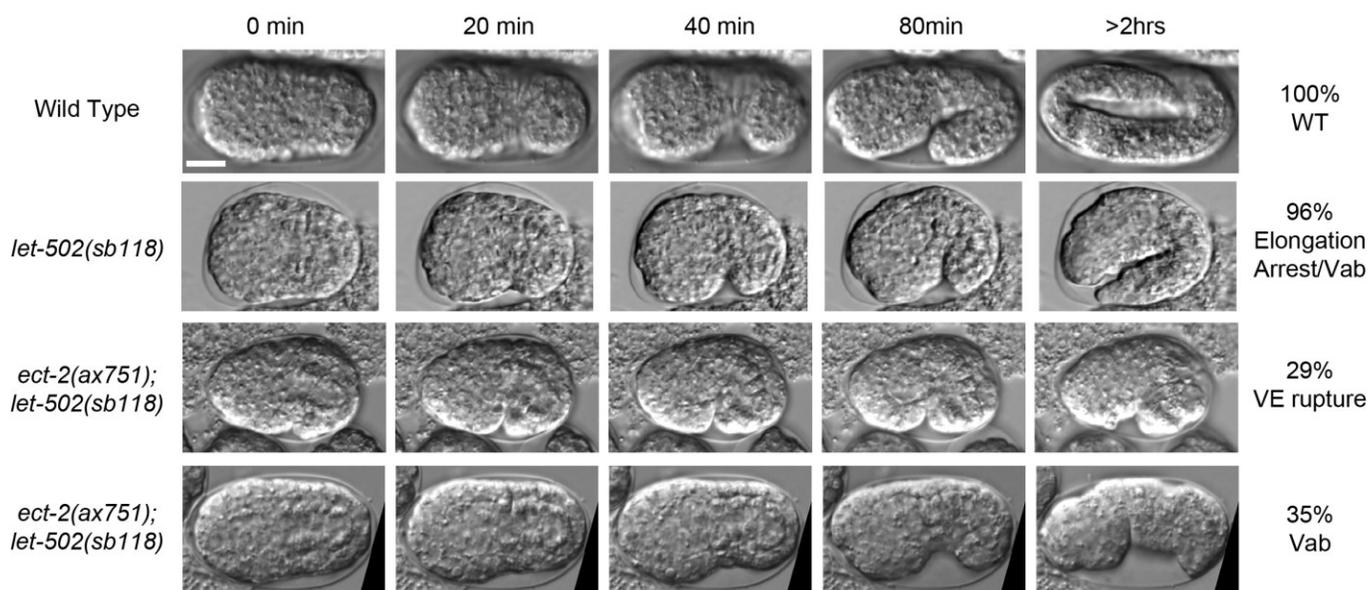
Figure 11. *ect-2* likely functions in the Rho pathway. The top panel shows DIC images of N2 embryos going through ventral enclosure and elongation. Underneath is a *let-502* mutant embryo, which arrests during early-mid elongation. Double *let-502; ect-2* mutant embryos display ventral enclosure rupture and Vab phenotypes (their proportion is shown on the right). The scale bar is 10 um.

type embryos, we predicted that phenotypes might be alleviated in the double mutants. Indeed, we observed suppression of the total number of phenotypes, including partial suppression of the *rho-1* elongation phenotypes (Table 4). Although our preliminary data suggests that *ect-2* may work in the Rho pathway to regulate ventral enclosure, further studies are required to properly place *ect-2* in the pathway. In particular, imaging AJM-1:GFP in the double mutants with weak loss and gain of *ect-2* function should reveal if *ect-2* works in this pathway to mediate ventral epidermal cell migration.

3.2.2 *ect-2* may function in parallel with the Rac/Cdc-42 pathway

In other cell types, Ect2 regulates Rac activity for migration (van Impel et al., 2009; Kwiatkowska et al., 2012). Also, previous studies showed that a Rac-dependent pathway is required for ventral epidermal cell migration during ventral enclosure (Sawa et al., 2003; Patel et al., 2008; Bernadskaya et al., 2012). Ventral epidermal cells fail to migrate and no longer form actin-rich protrusions in embryos with mutations in Rac (CED-10) and its interacting proteins (GEX-2 and GEX-3) (Chen et al., 1996; Soto et al., 2002; Patel et al., 2008). Since this is the only pathway known to regulate epidermal cell migration, we determined if *ect-2* genetically interacts with Rac or other pathway components (Table 6). To do this, we crossed *ect-2(ax751)* with two different Rac alleles; *ced-10(n3246),* which contains a gain-of-function (gof) mutation, and *ced-10(n1993),* which contains a loss-of-function (lof) mutation (Shakir et al., 2006). We propose that if *ect-2* and *ced-10* are in the same pathway, then as the downstream target of ECT-2, the

Table 6 *ect-2* likely works in parallel with the Rac/Cdc-42 pathway to regulate VE.

Genotype	Temperature (ºC)	Embryonic Lethality%*	Expected lethality%	χ^2 p value	Effect**
N2	20	0	--	--	--
ect-2(ax751)	20	27	--	--	--
ced-10(n3246)	20	14	--	--	--
ced-10(n1993)	20	6.5	--	--	--
wsp-1(gm324)	20	12	--	--	--
ect-2(ax751); ced-10(n3246)	20	96	41	χ^2 =269 $p < 0.01$	Enhancement
ect-2(ax751); ced-10(n1993)	20	89	33.5	χ^2 =187 $p < 0.01$	Enhancement
ect-2(ax751); wsp-1(gm324)	20	85	39	χ^2 =140 $p < 0.01$	Enhancement

* Sample size is 100 < n < 600; since Vab only exists as a minor phenotype for *ect-2 (ax751)* and was not seen with the other alleles, it was not included in the table. Furthermore, since none of the alleles are maternal null, the expected phenotypes were determined by adding the % of phenotypes for each allele.

** Significance tested by Chi-squared analysis, $p < 0.01$ indicates a strong effect.

gof *ced-10* allele should suppress *ect-2* (or show gof phenotypes), while the lof

allele may show no change in lethality or enhancement (because neither allele is

null). Regardless of the *ced-10* allele, the double mutants displayed enhanced

embryonic lethality (Table 6).

WSP-1/WASP functions downstream of Cdc-42 to regulate Arp2/3 for cell

migration (Miki et al., 1998; Sawa et al., 2003). We also tested genetic

interactions between *ect-2* and *wsp-1* using the *gm324* allele, which contains a

deletion and is a strong lof or null allele (Withee et al., 2004). We observed

enhanced embryonic lethality with the *ect-2(ax751); wsp-1(gm324)* double

mutants compared to the single mutants (Table 6). This data supports that *ect-2*

and Rac function in different pathways during embryogenesis. However, imaging

should be done with the double mutant embryos to assay ventral enclosure-

specific phenotypes, since the enhanced lethality could arise from their roles in

other embryonic events.

3.3 *ect-2* regulates the accumulation of non-muscle myosin during ventral enclosure

3.3.1 Myosin organizes supracellularly during ventral enclosure

The Rho pathway typically regulates myosin contractility during different

types of tissue morphogenesis in metazoans (Brock et al., 1996; Roh-Johnson et

al., 2012). *C. elegans* ventral enclosure is another type of morphogenetic event,

and shares some features with dorsal closure in *Drosophila*, which is known to

be a myosin-dependent process. Since myosin has not been previously studied

in ventral enclosure, we imaged a recently generated NMY-2:GFP strain during

mid-embryogenesis. This strain was made using the CRISPR system to place

NMY-2:GFP at the *nmy-2* locus, and shows consistently higher expression levels

compared to a previously made NMY-2:GFP *zuIs45* strain (Dickinson et al.,

2013). Our imaging studies revealed that myosin foci coalesce into a

supracellular structure along the margin of the ventral epidermal cells as they

migrate in toward the ventral midline (Figure 12). At the beginning of ventral

enclosure, myosin foci are more loosely organized, but as the epidermal cells

migrate toward the ventral midline, the foci aggregate into a circular structure,

which becomes a single line as cells adhere at the ventral midline (Figure 12).

This data shows that nonmuscle myosin is highly organized during ventral

enclosure, consistent with our findings that *rho-1* and *ect-2* (key regulators of

myosin contractility) are required for ventral epidermal cell migration.

3.3.2 *ect-2* regulates coalescent of myosin during ventral enclosure

Next, I determined if *ect-2* is required for the enrichment and organization

of myosin into a ring during ventral enclosure. I generated a strain with *ect-2(ax751)*; NMY-2:GFP and imaged embryos during development. In mutant

embryos that displayed strong ventral enclosure phenotypes, there were fewer

myosin foci, and these foci were not well-organized during ventral enclosure

(Figure 13A). In mutant embryos that displayed delays in ventral enclosure, the

myosin foci were less enriched in comparison to control embryos, and the ring

appeared to be less organized. *ect-2(ax751)*; NMY-2:GFP that exhibited no
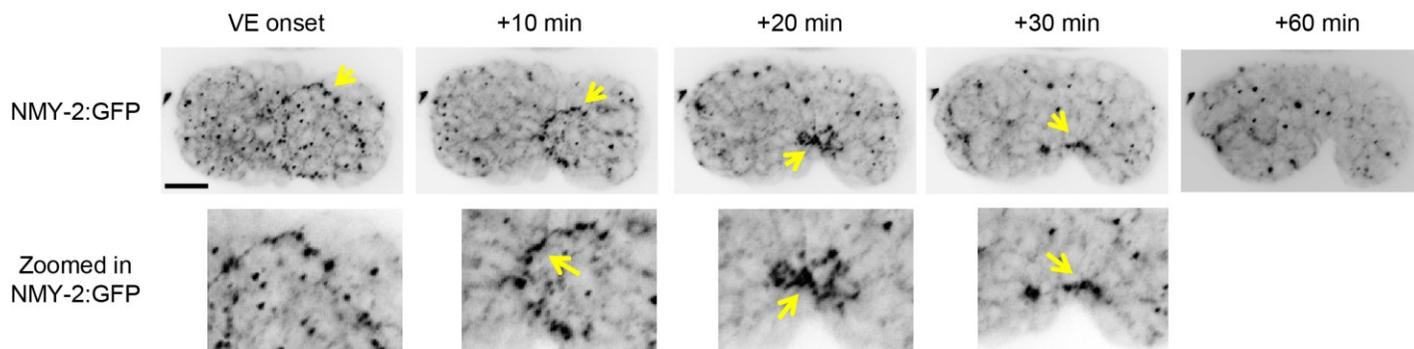
Figure 12. Non-muscle myosin accumulates as foci along the margins of ventral epidermal cells and coalesces into a supracellular structure during ventral enclosure. Live imaging of NMY-2:GFP embryos show NMY-2:GFP localization to foci along the margin of ventral epidermal cells, which coalesces as cells meet at the ventral midline (n = 9). Underneath are zoomed in images of regions highlighting the pattern of accumulation and coalescence (yellow arrows). The scale bar is 10 um.

.
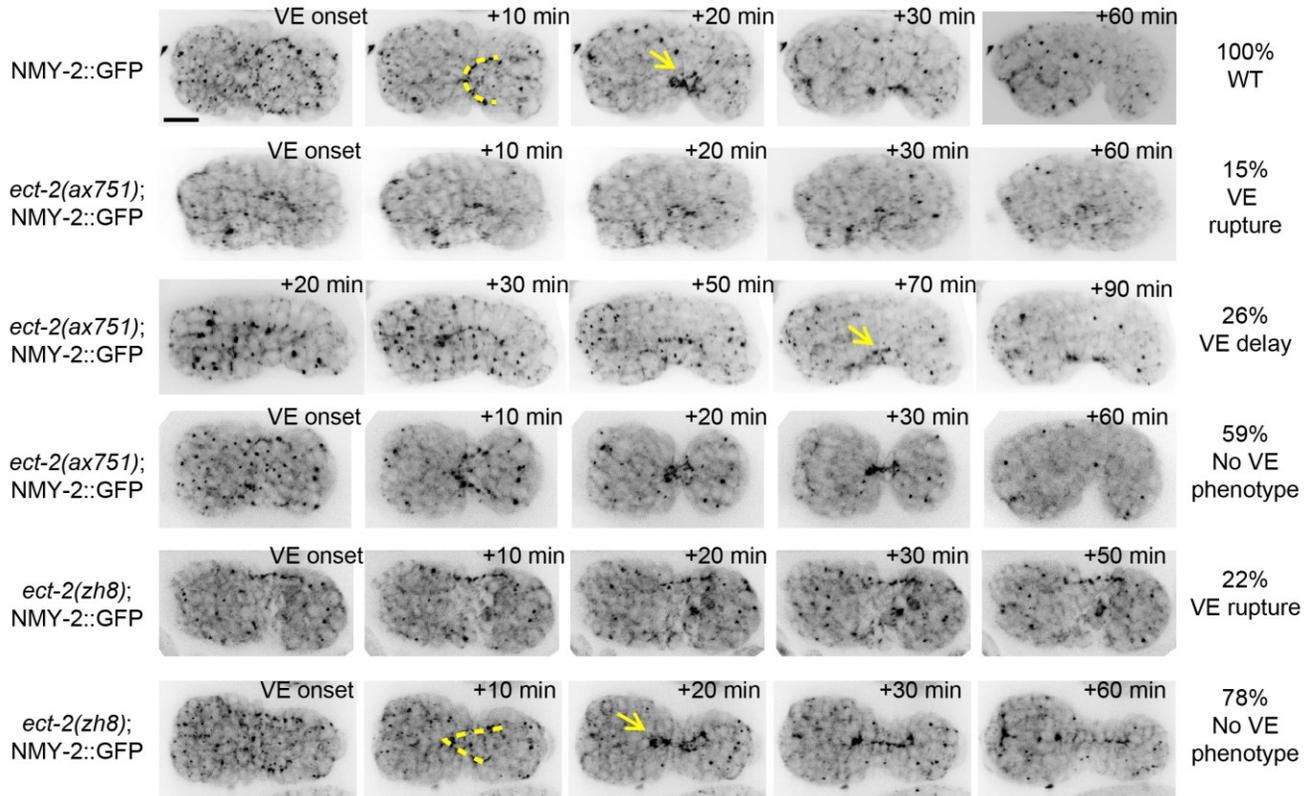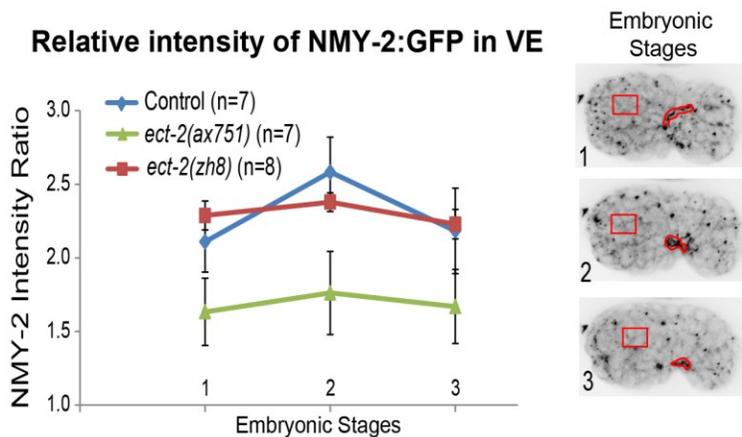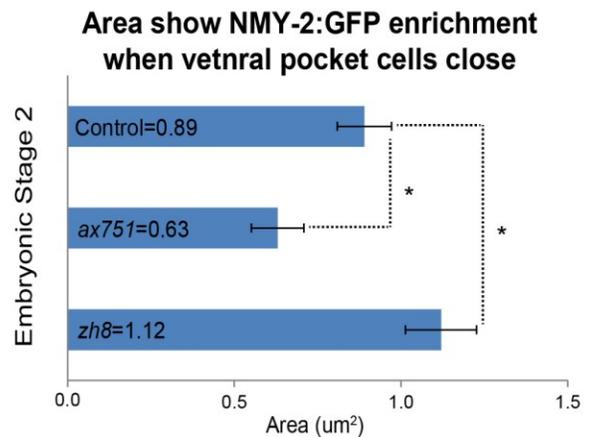
Figure 13. *ect-2* regulates the organization of myosin into supracellular structures during ventral enclosure. (A) Images show NMY-2:GFP in control and *ect-2* mutant embryos through ventral enclosure. The yellow arrow points to NMY-2 accumulation into a supracellular structure. The dashed line shows the pattern of foci as they initially coalesce. (B) A graph shows measurements of the ratio of average NMY-2 intensity in the coalesced regions (red ROI's), compared to average background intensity (red box). Three time points were measured, as indicated by the embryos on the right. Bars show standard deviations. (C) A graph shows the total area (in um^2) of coalesced NMY-2:GFP signal at embryonic stage 2' (see pictures of embryos in B). Bars show standard deviation. The student t-test was used to calculate significance, *$p<0.01$. The scale bar is 10 um.

ventral enclosure phenotype had similar myosin distribution patterns as control embryos (Figure 13A). I also generated a strain with *ect-2 (zh8)*; NMY-2:GFP to determine if increasing ECT-2 activity also affects the organization of myosin (Figure 13A). Although some of these embryos ruptured during early ventral enclosure, in other embryos I saw that myosin formed into a "V" shape rather than the circular "C" shape that was prominent in control embryos (Figure 13A). Then, I quantitated the average intensity of NMY-2:GFP at sites of enrichment in comparison to background during 3 different time points of ventral enclosure, to assess changes in myosin over time (Figure 13B). In control embryos, the ratio of NMY-2:GFP was above 2.1 during ventral enclosure; and showed a peak value of 2.5, just prior to closure of the ventral pocket cells at the midline (n = 7). In *ect-2(ax751)* mutant embryos, the ratio of NMY-2:GFP was below 1.6 in all stages, and there was no obvious peak in intensity when ventral pocket cells met at the ventral midline (n = 6). In *ect-2(zh8)* embryos, the ratio of NMY-2:GFP intensity was high, similar to control levels, but there was no peak when the ventral pocket cells closed (n = 8). Interestingly, although *ect-2(zh8)* embryos had no extra myosin accumulation within the same regions as control embryos, we noticed that myosin enrichment occurred over a broader area (Figure 13A). Quantification of total area with myosin enrichment from embryos during late ventral enclosure, when the supracellular structure was more obvious in control embryos, revealed that area with myosin enrichment was increased in *ect-2(zh8)* mutant embryos compared to control embryos (n = 8), and decreased in *ect-2(ax751)* embryos (n = 7, Figure 13C). This data supports our previous finding

that *ect-2* likely works in the Rho pathway to regulate myosin contractility for ventral epidermal cell migration.

3.4 *ect-2* may regulate adherens junctions

The formation and stability of adherens junctions is also important for successful ventral enclosure. Embryos with mutations in adherens junction proteins are unable to form or maintain new junctions, and display ventral enclosure phenotypes or are Vab (Costa et al., 1998; Koppen et al., 2001; Labouesse, 2006). In mammalian cells, Ect2 regulates adherens junctions through a RhoA pathway, and Ect2 depletion causes a decrease in the levels of myosin at the junctions, and destabilizes cadherin (Ratheesh et al., 2012). We also determined if *ect-2* is required for the formation or maintenance of new junctions during ventral enclosure. *hmp-2* encodes beta-catenin, part of the catenin-cadherin complex, and *qm39* is a weak lof allele that displays low embryonic lethality, and has Vab phenotypes (Figure 14; Tables 7, 8) (Lockwood et al., 2008). There was no change in embryonic lethality in *ect-2(ax751); hmp-2(qm39)* double mutant embryos compared to the single mutants (Table 7). We imaged embryos during development and found that the percentage of ruptured embryos during ventral enclosure, and larva with Vab phenotypes was not significantly changed in the double mutant compared to the single mutants (Figure 14; Table 8). Although more components of the junction should be tested to determine if *ect-2* is involved in junctions, our data supports that beta-catenin and *ect-2* could function in the same pathway for similar embryonic events.

55
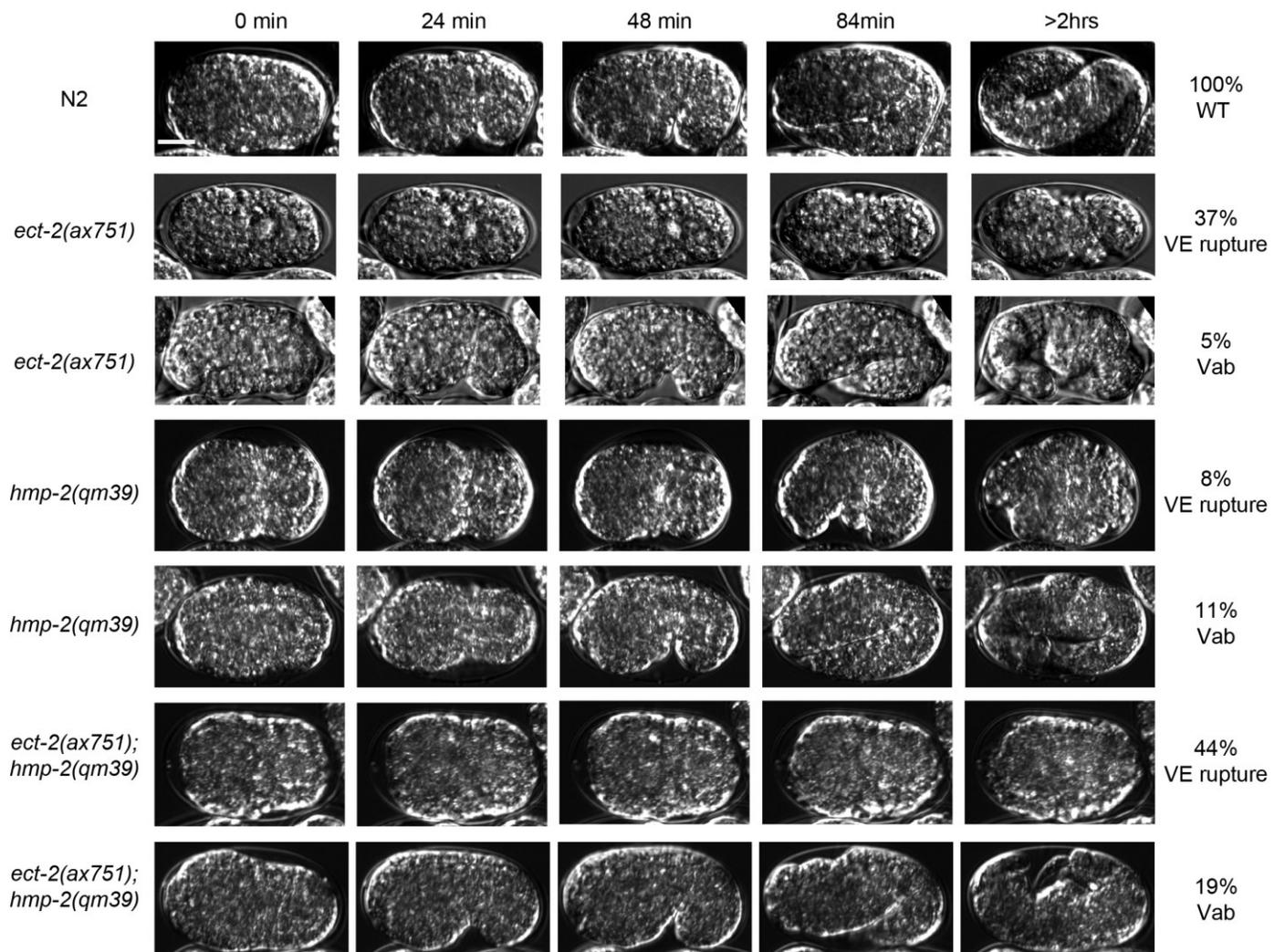
Figure 14. *ect-2* may regulate adherens junctions. The panels show DIC images of N2 (wild-type), single mutant *ect-2(ax751)* and *hmp-2(qm39)* embryos; and double mutant embryos through ventral enclosure and elongation. The proportion of each phenotype is shown on the right, 30<n<60 for each genotype. The scale bar is 10 um.

Table 7 *ect-2* **may regulate adherens junctions.**

Genotype	Temperature (^{0}C)	Embryonic Lethality%*	Expected lethality%	χ^2 p value	Effect**
N2	20	0	--	--	--
ect-2(ax751)	20	27.5	--	--	--
hmp-2(qm39)	20	1.5	--	--	--
ect-2(ax751); hmp-2(qm39)	20	33.9	29	χ^2 =1.39 $p > 0.05$	No effect

* Sample size is 200 < n < 300. Expected lethality was determined by adding the proportion of phenotypes for each allele, since neither is maternal null.

** Significance tested by Chi-squared analysis, $p > 0.05$ indicates no effect.

Table 8 *ect-2* **may be involved in adherens junctions regulation.**

Genotype*	Before VE%	VE Rupture%	Vab%	Delay%
N2	0	0	0	0
ect-2(ax751)	16.1	37.1	5	14.5
hmp-2(qm39)	0	7.9	10.5	0
ect-2(ax751); hmp-2(qm39)	7.4	43.9	19.3	0

* Sample size for each genotype is 30 < n < 60.

However, since neither allele is a null, we have to repeat these studies using different allelic combinations.

Chapter 4. Discussion

In this thesis we show that *ect-2,* which encodes a RhoGEF, is required for multiple migratory events during *C. elegans* embryogenesis, including neuroblast migration for ventral cleft closure, and epidermal migration for ventral enclosure. During ventral cleft closure, neuroblasts migrate to close a depression left on the ventral surface of the embryo after gastrulation. During ventral enclosure, ventral epidermal cells migrate and adhere at the ventral midline to enclose the embryo in a single layer of epidermal cells. Our genetic data suggests that *ect-2* may regulate myosin contractility to mediate migratory events. Moreover, *ect-2* may regulate the formation or stability of cell-cell junctions during ventral enclosure.

4.1 *ect-2* is required for neuroblast migration

We found that *ect-2* is required for the migration of neuroblasts during ventral cleft closure (Figure 7). Neuroblasts serve as a substrate for the migration of overlying ventral epidermal cells during ventral enclosure, and mis-positioned neuroblasts can cause ventral enclosure defects (Chin-Sang et al., 1999; Chin-Sang et al., 2002; Ikegami et al., 2012). We found that ECT-2 is enriched in the majority of neuroblasts, where it localizes to cell boundaries (Figure 9). Furthermore, in *ect-2* mutant embryos, we observed persistent and misplaced ventral clefts, which resulted in phenotypes in ventral enclosure (Figure 7). These data support a role for *ect-2* in regulating the migration of neuroblasts. However, defects in ventral cleft closure could also arise due to abnormal neuroblast division. To determine if *ect-2* is required for neuroblast cytokinesis, live imaging

60

will be performed using *ect-2 (ax751)* mutant embryos co-expressing a

fluorescent-labeled neuroblast-specific marker, and a second marker for the

membrane that will allow us to visualize their division *in vivo* (Fotopoulos et al.,

2013). This experiment will also help us determine if neuroblast cell shape or

organization is altered in the *ect-2* mutant embryos. Since *ect-2(ax751)* embryos

have few cytokinesis defects in the early embryo (Zonies et al., 2010), and

tissues are formed similar to wild-type embryos, we propose that *ect-2* mediates

neuroblast migration vs. their division.

4.2 *ect-2* is required for ventral enclosure

In addition to regulating neuroblast migration *ect-2* is required for ventral

enclosure during later stages of embryogenesis (Figure 6). ECT-2 localizes to the

boundaries of epidermal cells in a pattern reminiscent of RHO-1, and is required

for their migration (Figure 9) (Fotopoulos et al., 2013). Despite the range in

severity of ventral enclosure phenotypes (*e.g.* delay vs. rupture) in *ect-2* mutant

embryos, ventral epidermal cells took twice as long to migrate in comparison to

wild-type cells (Figure 8). In addition, the pattern of cell migration was quite

different in comparison to wild-type embryos. For example, in some of the *ect-2*

mutant embryos, the leading cells met at the same time or even later than the

ventral pocket cells (Figure 8). This data suggests that ECT-2 mediates the

migration of ventral epidermal cells by directly regulating their cytoskeletal

dynamics, or by influencing their dynamics from the underlying neuroblasts.

There are several ways that ECT-2 could affect migration, either

autonomously, or non-autonomously. First, the leading cells migrate via actin-rich

protrusions that point toward the ventral midline, and ECT-2 could regulate Rac or Cdc42 to mediate the formation of these protrusions. Second, the ventral pocket cells have actin cables that form at the cell margins to form a ring, and ECT-2 could regulate the formation of F-actin for this ring, or the closure of this ring via a contractile, purse-string mechanism (Williams-Masson et al., 1997). Furthermore, in both leading and pocket cells, ECT-2 could regulate cell shape changes that are also required for these cells to migrate. Genetic crosses between *ect-2(ax751)* and components of the *rho-1* pathway suggests that they function in the same pathway, and we favour a role for ECT-2 in regulating actomyosin contractility for ventral enclosure. This role may not be restricted to the epidermis, and ECT-2 could also regulate contractility within the neuroblasts during ventral enclosure. In *Drosophila*, the amnioserosa could function similar to neuroblasts, since they are required for closure of the epidermis on the dorsal surface of the embryo (Jacinto et al., 2002). Interestingly, this tissue has extensive actomyosin contractility, which helps organize actomyosin contractility in the overlying epidermal cells to mediate effective closure (Kiehart et al., 2000; Franke et al., 2005). Therefore, *ect-2,* in addition to regulating neuroblast migration, could also regulate myosin contractility in the neuroblasts to coordinate the formation of a supracellular structure that closes the ventral pocket.

Since *ect-2* is required for cytokinesis, it is possible that the ventral enclosure phenotype in *ect-2* mutant embryos is due to an insufficient number of epidermal cells. However, there was no difference in the number of epidermal cells in wild-

type vs. *ect-2* mutant embryos, suggesting that *ect-2* mediates epidermal cell migration without affecting epidermal cytokinesis. The *ect-2* mutant allele used in this study seems to preferentially give rise to multiple migration defects instead of cell division defects. Therefore, we propose that different levels of ECT-2 are required to carry out different events (Figure 15). Lowering ECT-2 below a threshold could permit ECT-2 to regulate cytokinesis, but not migration, and if ECT-2 is drops to even lower levels, then both cytokinesis and migration are blocked (Jantsch-Plunger et al., 2000; Loria et al., 2012).

4.3 *ect-2* likely functions in the Rho pathway for myosin contractility

Our data suggests that *ect-2* functions in the Rho pathway to regulate cell migration. As described earlier, *ect-2* similarly functions in the Rho pathway for the division and migration of P-cells during later stages of development (Morita et al., 2005). We observed ventral enclosure phenotypes in *rho-1* mutant embryos, and RHO-1 localizes to epidermal cell boundaries with a pattern similar to ECT-2 (Figures 9). In addition, our genetic studies support that *ect-2* could function in the Rho pathway (Figures 10, 11; Table 4). Double mutants between *ect-2* and Rho pathway components showed no enhancement of total phenotypes. We also found shifts in phenotypes depending on the allelic combination. For example, we saw that some of the rupture phenotypes were suppressed in *let-502; ect-2* mutant embryos. We propose that weakened myosin contractility in the
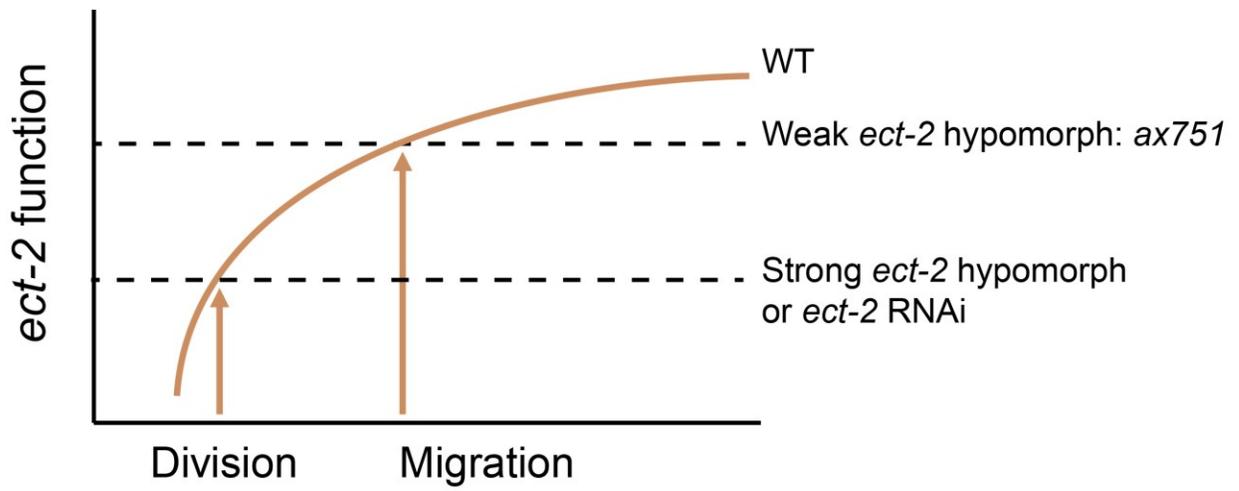
Figure 15. Model for the threshold requirements of *ect-2* during embryogenesis. For example, while low levels of *ect-2* are sufficient to mediate cytokinesis, they are not sufficient to mediate migration.

neighboring lateral epidermal cells puts less pressure on the embryo and prevents the extrusion of internal contents during later stages of development. Interestingly, the double mutant larva had strong Vab phenotypes suggesting that ventral enclosure was still defective. We also saw suppression of phenotypes between the gof *ect-2* allele, and the null *rho-1* allele. Although the *rho-1* allele was not maternal, making it difficult to properly assess a 'pathway' with *rho-1* or *ect-2* downstream, the alleviation of ventral enclosure phenotypes coupled with the alleviation of elongation phenotypes supports that they could function in the same pathway. However, the different phenotypes observed in the double mutant combinations need to be better assessed by performing live imaging experiments. In particular, using AJM-1:GFP to image the migration rates of the ventral epidermal cells will help us determine 'enhancement' or 'suppression' of ventral enclosure phenotypes.

Our data also suggests that *ect-2* does not function in the Rac/Cdc-42 pathway to regulate migration. Rac activates the Wave/Scar and Arp2/3 complexes to promote the nucleation of short, branched actin to form protrusions for epidermal cell migration, and mutations in this pathway cause Gex (rupture) phenotypes (Patel et al., 2008; Shakir et al., 2008). Double mutants generated between *ect-2* and Rac pathway components showed enhanced embryonic lethality (Table 6). Therefore, *ect-2* works in parallel to the Rac pathway to regulate ventral enclosure. However, we cannot completely rule out a function for *ect-2* in the Rac pathway, since all of the alleles we tested were hypomorphs. However, *ect-2(ax751)* displayed enhanced embryonic lethality when combined

with a gof Rac allele. We predict that if ECT-2 functions as a GEF for Rac, then embryos should display Rac gof phenotypes, regardless of whether or not its GEF is functional. However, since *ect-2* and Rac could regulate multiple events during embryogenesis, the double mutant embryos will have to be analyzed specifically during ventral enclosure to properly determine if they are in parallel pathways. Since we also have data that supports a role for *ect-2* in the Rho pathway, we suggest that *ect-2* functions in the Rho pathway, and works in parallel to the Rac pathway. Rho and Rac typically work antagonistically to regulate migration in other cell types; while Rac regulates the formation of short, branched F-actin at the front of the cell to form lamellopodia, RhoA regulates the formation of stress fibers and generates contractility in the rear of the cell to push the cell forward (D'Avino et al., 2004; Shoval and Kalcheim, 2012). In *C. elegans*, Rho and Rac pathways also work antagonistically across different tissues or cell types. For example, during embryonic elongation, *rho-1* is required to regulate myosin contractility within the lateral epidermal cells to mediate their cell shape changes, while Rac regulates myosin relaxation in the dorsal and ventral epidermal cells (Piekny et al., 2000). Therefore, we favor the hypothesis that *ect-2* works in the Rho pathway to regulate actomyosin events (either in the neuroblasts or in the epidermal cells) for ventral enclosure, while the Rac/Cdc-42 pathway regulates the formation of actin-rich protrusions to mediate ventral epidermal cell migration.

4.4 *ect-2* regulates the localization of non-muscle myosin during ventral enclosure

Myosin contractility is required for the migration of many cell types, but it had not been shown to have a role in ventral enclosure (Vicente-Manzanares et al., 2009). Using embryos expressing NMY-2:GFP, we saw the accumulation of myosin foci at the margins of migrating ventral epidermal cells in a ring-like pattern, which aggregated into a supracellular structure as the cells approached the ventral midline (Figure 12). Previous studies showed that thick actin cables similarly form along the border of migrating ventral pocket cells. Laser ablation caused these cells to immediately retract, suggesting that they were under tension (Williams-Masson et al., 1997). Since myosin is the motor protein that generates contractile forces, our data is consistent with these earlier studies and suggests that a contractile ring forms around the border of the ventral pocket cells, which contracts like a purse-string to mediate their closure.

Our data suggests that *ect-2* functions in the Rho pathway, and we predict that it regulates myosin activity. Consistent with this prediction, we observed a decrease in the intensity of myosin localization in *ect-2(ax751)* embryos expressing NMY-2:GFP. Embryos that had weak, or no ventral enclosure phenotypes were similar to control embryos, while embryos that had strong delays or rupture phenotypes had low levels of myosin, which failed to form an organized supracellular structure. Furthermore, we also saw a mild up-regulation of myosin accumulation in embryos with the *ect-2* gof allele, and the pattern of myosin was different in comparison to control cells (Figure 13). This data supports our hypothesis that *ect-2* regulates myosin contractility (either in the neuroblasts or in the epidermal cells) for ventral enclosure.

67

However, it is not clear how *ect-2* affects migration of the leading cells, which rely more on their protrusions for migration. In other cell types, myosin contractility provides forces that contribute to migration. For example, myosin regulates adhesion, as well as the formation and contraction of stress fibers to push the cell forward (Giannone et al., 2007; Vicente-Manzanares et al., 2009). Myosin could also contribute to the stability and/or retraction of protrusions that mediate cell migration. Since *ect-2* could regulate myosin, it could influence any one of these events to regulate the migration of the leading cells in ventral enclosure. We favor the hypothesis that myosin generates forces in either the epidermis and/or neuroblasts to coordinate the formation and closure of a supracellular contractile ring by a purse-string mechanism.

4.5 *ect-2* may regulate adherens junctions

Adhesion keeps neighboring cells together during tissue morphogenesis, and connects contralateral cell pairs. This is partly mediated by adherens junctions, which are regulated by Rho signaling (Chisholm and Hardin, 2005; Vicente-Manzanares et al., 2009; Martin et al., 2010). *C. elegans* embryos with mutations in adherens junction components have ventral enclosure phenotypes (Costa et al., 1998; Koppen et al., 2001). Since Rho regulates adherens junctions in other organisms, we performed genetic studies with *ect-2(ax751)* and adherens junctions alleles. We found that embryonic lethality was not enhanced in the double mutants, suggesting that they function in the same pathway (Table 7). We also found that the double mutant embryos showed similar proportions of ventral enclosure phenotypes, further supporting that they function in the same pathway

68

(Figure 14, Table 8). In mammalian cell-cell junctions, catenins recruit Ect2 and locally activate Rho signaling pathway to regulate junction integrity through myosin (Ratheesh et al., 2012).

Based on studies performed in this thesis, we propose a working model for cell migration during ventral enclosure, which includes *ect-2*, myosin, adherens junctions, and neuroblasts (Figure 16). In wild-type embryos, well-organized neuroblasts provide a substrate for the migration of overlying epidermal cells. They could provide chemical and/or mechanical cues that maintain the direction and efficiency of their migration. As the actomyosin filaments accumulate at the margins of epidermal cells and aggregate into a supracellular ring-like structure, the neuroblasts could also contribute to this organization by either providing some of their own active myosin filaments, or by forming a template for the ring. In all of the ventral epidermal cells, myosin contractility likely regulates the apical constriction of these cells and their extension toward the ventral midline. Also, adherens junctions formed between neighboring cells keep the cells connected so that they migrate as a unit, and connect the contralateral pairs after closure. In *ect-2* mutants, neuroblasts are not well-organized, making the migration of epidermal cells less efficient. In addition, there are lower levels of myosin contractility in either the neuroblasts or epidermal cells, which could impede the formation of a well-organized supracellular ring, and make adherens junctions unstable.
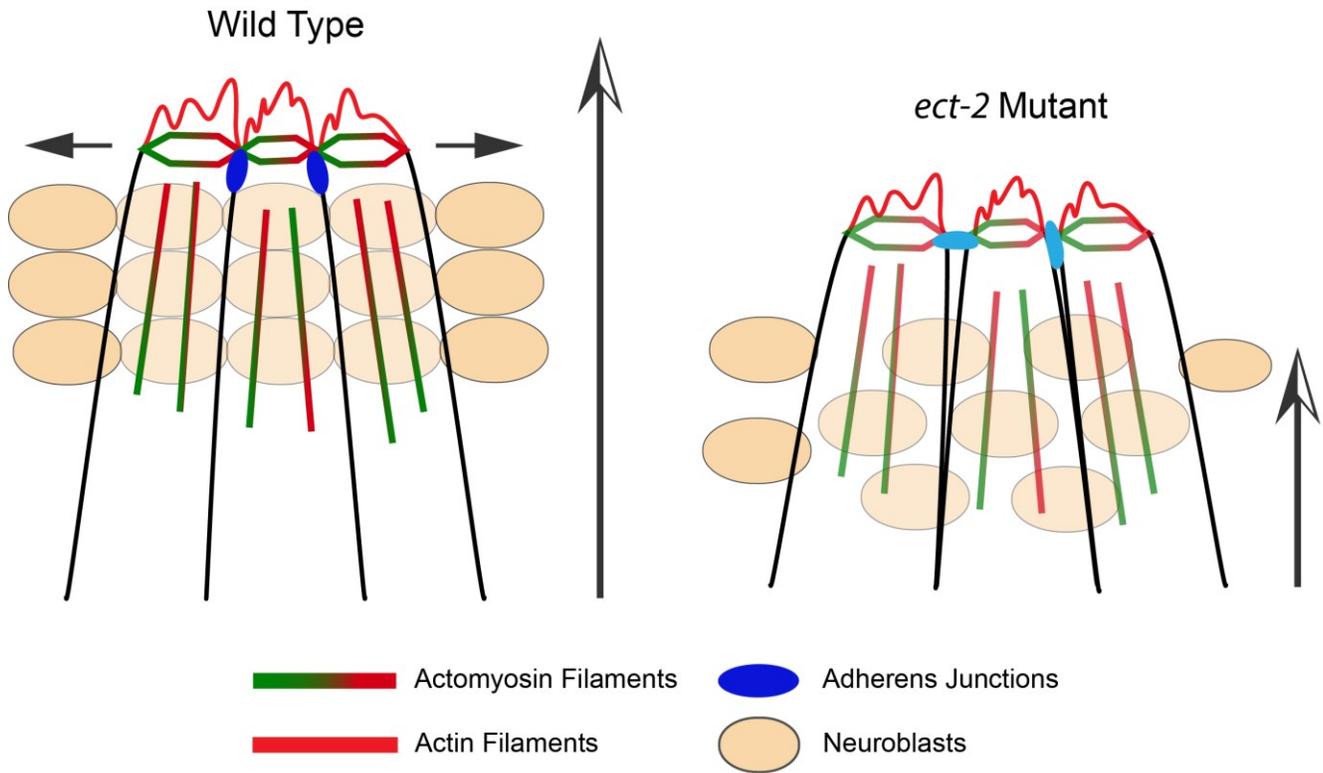
Figure 16. A cartoon model shows how *ect-2* regulates ventral enclosure. *ect-2* is required to stabilize the organization of myosin filaments into an organized supracellular structure around the margins of the ventral epidermal cells. The underlying nueroblasts also require *ect-2* for their proper localization and arrangement to ensure embryogenesis. In addition, it may stabilize the adherens junctions between neighboring epidermal cells, and between contralateral cell pairs.

Reference

Bement, W.M., Forscher, P., Mooseker, M.S., 1993. A novel cytoskeletal structure involved in purse string wound closure and cell polarity maintenance. The Journal of cell biology 121, 565-578.

Bernadskaya, Y.Y., Wallace, A., Nguyen, J., Mohler, W.A., Soto, M.C., 2012. UNC-40/DCC, SAX-3/Robo, and VAB-1/Eph polarize F-actin during embryonic morphogenesis by regulating the WAVE/SCAR actin nucleation complex. PLoS genetics 8, e1002863.

Bompard, G., Sharp, S.J., Freiss, G., Machesky, L.M., 2005. Involvement of Rac in actin cytoskeleton rearrangements induced by MIM-B. Journal of cell science 118, 5393-5403.

Brenner, S., 1974. The genetics of Caenorhabditis elegans. Genetics 77, 71-94.

Brock, J., Midwinter, K., Lewis, J., Martin, P., 1996. Healing of incisional wounds in the embryonic chick wing bud: characterization of the actin purse-string and demonstration of a requirement for Rho activation. The Journal of cell biology 135, 1097-1107.

Canevascini, S., Marti, M., Frohli, E., Hajnal, A., 2005. The Caenorhabditis elegans homologue of the proto-oncogene ect-2 positively regulates RAS signalling during vulval development. EMBO reports 6, 1169-1175.

Chan, E., Nance, J., 2013. Mechanisms of CDC-42 activation during contact-induced cell polarization. Journal of cell science 126, 1692-1702.

Chen, W., Chen, S., Yap, S.F., Lim, L., 1996. The Caenorhabditis elegans p21-activated kinase (CePAK) colocalizes with CeRac1 and CDC42Ce at hypodermal cell boundaries during embryo elongation. The Journal of biological chemistry 271, 26362-26368.

Chin-Sang, I.D., Chisholm, A.D., 2000. Form of the worm: genetics of epidermal morphogenesis in C. elegans. Trends in genetics : TIG 16, 544-551.

Chin-Sang, I.D., George, S.E., Ding, M., Moseley, S.L., Lynch, A.S., Chisholm, A.D., 1999. The ephrin VAB-2/EFN-1 functions in neuronal signaling to regulate epidermal morphogenesis in C. elegans. Cell 99, 781-790.

Chin-Sang, I.D., Moseley, S.L., Ding, M., Harrington, R.J., George, S.E., Chisholm, A.D., 2002. The divergent C. elegans ephrin EFN-4 functions inembryonic morphogenesis in a pathway independent of the VAB-1 Eph receptor. Development 129, 5499-5510.

Chisholm, A.D., Hardin, J., 2005. Epidermal morphogenesis. WormBook : the online review of C. elegans biology, 1-22.

Costa, M., Raich, W., Agbunag, C., Leung, B., Hardin, J., Priess, J.R., 1998. A putative catenin-cadherin system mediates morphogenesis of the Caenorhabditis elegans embryo. The Journal of cell biology 141, 297-308.

D'Avino, P.P., Savoian, M.S., Glover, D.M., 2004. Mutations in sticky lead to defective organization of the contractile ring during cytokinesis and are enhanced by Rho and suppressed by Rac. The Journal of cell biology 166, 61-71.

Dechant, R., Glotzer, M., 2003. Centrosome separation and central spindle assembly act in redundant pathways that regulate microtubule density and trigger cleavage furrow formation. Developmental cell 4, 333-344.

Dickinson, D.J., Ward, J.D., Reiner, D.J., Goldstein, B., 2013. Engineering the Caenorhabditis elegans genome using Cas9-triggered homologous recombination. Nature methods 10, 1028-1034.

Dvorsky, R., Ahmadian, M.R., 2004. Always look on the bright site of Rho: structural implications for a conserved intermolecular interface. EMBO reports 5, 1130-1136.

Fields, A.P., Justilien, V., 2010. The guanine nucleotide exchange factor (GEF) Ect2 is an oncogene in human cancer. Advances in enzyme regulation 50, 190-200.

Fotopoulos, N., Wernike, D., Chen, Y., Makil, N., Marte, A., Piekny, A., 2013. Caenorhabditis elegans anillin (ani-1) regulates neuroblast cytokinesis and epidermal morphogenesis during embryonic development. Developmental biology 383, 61-74.

Franke, J.D., Montague, R.A., Kiehart, D.P., 2005. Nonmuscle myosin II generates forces that transmit tension and drive contraction in multiple tissues during dorsal closure. Current biology : CB 15, 2208-2221.

George, S.E., Simokat, K., Hardin, J., Chisholm, A.D., 1998. The VAB-1 Eph receptor tyrosine kinase functions in neural and epithelial morphogenesis in C. elegans. Cell 92, 633-643.

Giannone, G., Dubin-Thaler, B.J., Rossier, O., Cai, Y., Chaga, O., Jiang, G., Beaver, W., Dobereiner, H.G., Freund, Y., Borisy, G., Sheetz, M.P., 2007. Lamellipodial actin mechanically links myosin activity with adhesion-site formation. Cell 128, 561-575.

Glavis-Bloom, J., Muhammed, M., Mylonakis, E., 2012. Of model hosts and man: using Caenorhabditis elegans, Drosophila melanogaster and Galleria mellonella as model hosts for infectious disease research. Advances in experimental medicine and biology 710, 11-17.

Goode, B.L., Eck, M.J., 2007. Mechanism and function of formins in the control of actin assembly. Annual review of biochemistry 76, 593-627.

Harrington, R.J., Gutch, M.J., Hengartner, M.O., Tonks, N.K., Chisholm, A.D., 2002. The C. elegans LAR-like receptor tyrosine phosphatase PTP-3 and the VAB-1 Eph receptor tyrosine kinase have partly redundant functions in morphogenesis. Development 129, 2141-2153.

Ikegami, R., Simokat, K., Zheng, H., Brown, L., Garriga, G., Hardin, J., Culotti, J., 2012. Semaphorin and Eph receptor signaling guide a series of cell movements for ventral enclosure in C. elegans. Current biology : CB 22, 1-11.

Jacinto, A., Woolner, S., Martin, P., 2002. Dynamic analysis of dorsal closure in Drosophila: from genetics to cell biology. Developmental cell 3, 9-19.

Jankovics, F., Henn, L., Bujna, A., Vilmos, P., Kiss, N., Erdelyi, M., 2011. A functional genomic screen combined with time-lapse microscopy uncovers a novel set of genes involved in dorsal closure of Drosophila embryos. PloS one 6, e22229.

Jantsch-Plunger, V., Gonczy, P., Romano, A., Schnabel, H., Hamill, D., Schnabel, R., Hyman, A.A., Glotzer, M., 2000. CYK-4: A Rho family gtpase activating protein (GAP) required for central spindle formation and cytokinesis. The Journal of cell biology 149, 1391-1404.

Jenkins, N., Saam, J.R., Mango, S.E., 2006. CYK-4/GAP provides a localized cue to initiate anteroposterior polarity upon fertilization. Science 313, 1298-1301.

Kiehart, D.P., Galbraith, C.G., Edwards, K.A., Rickoll, W.L., Montague, R.A., 2000. Multiple forces contribute to cell sheet morphogenesis for dorsal closure in Drosophila. The Journal of cell biology 149, 471-490.

Koppen, M., Simske, J.S., Sims, P.A., Firestein, B.L., Hall, D.H., Radice, A.D., Rongo, C., Hardin, J.D., 2001. Cooperative regulation of AJM-1 controls junctional integrity in Caenorhabditis elegans epithelia. Nature cell biology 3, 983-991.

Kwiatkowska, A., Didier, S., Fortin, S., Chuang, Y., White, T., Berens, M.E., Rushing, E., Eschbacher, J., Tran, N.L., Chan, A., Symons, M., 2012. The small GTPase RhoG mediates glioblastoma cell invasion. Molecular cancer 11, 65.

Labouesse, M., 2006. Epithelial junctions and attachments. WormBook : the online review of C. elegans biology, 1-21.

Lee, J.Y., Goldstein, B., 2003. Mechanisms of cell positioning during C. elegans gastrulation. Development 130, 307-320.

Lim, J., Thiery, J.P., 2012. Epithelial-mesenchymal transitions: insights from development. Development 139, 3471-3486.

Lin, L., Tran, T., Hu, S., Cramer, T., Komuniecki, R., Steven, R.M., 2012. RHGF-2 is an essential Rho-1 specific RhoGEF that binds to the multi-PDZ domain scaffold protein MPZ-1 in Caenorhabditis elegans. PloS one 7, e31499.

Lockwood, C., Zaidel-Bar, R., Hardin, J., 2008. The C. elegans zonula occludens ortholog cooperates with the cadherin complex to recruit actin during morphogenesis. Current biology : CB 18, 1333-1337.

Loria, A., Longhini, K.M., Glotzer, M., 2012. The RhoGAP domain of CYK-4 has an essential role in RhoA activation. Current biology : CB 22, 213-219.

Loveless, T., Hardin, J., 2012. Cadherin complexity: recent insights into cadherin superfamily function in C. elegans. Current opinion in cell biology 24, 695-701.

Lu, Y., Settleman, J., 1999. The Drosophila Pkn protein kinase is a Rho/Rac effector target required for dorsal closure during embryogenesis. Genes & development 13, 1168-1180.

Magie, C.R., Pinto-Santini, D., Parkhurst, S.M., 2002. Rho1 interacts with p120ctn and alpha-catenin, and regulates cadherin-based adherens junction components in Drosophila. Development 129, 3771-3782.

Mains, P.E., Kemphues, K.J., Sprunger, S.A., Sulston, I.A., Wood, W.B., 1990. Mutations affecting the meiotic and mitotic divisions of the early Caenorhabditis elegans embryo. Genetics 126, 593-605.

Martin, A.C., Gelbart, M., Fernandez-Gonzalez, R., Kaschube, M., Wieschaus, E.F., 2010. Integration of contractile forces during tissue invagination. The Journal of cell biology 188, 735-749.

Martin, P., Lewis, J., 1992. Actin cables and epidermal movement in embryonic wound healing. Nature 360, 179-183.

Matsumura, F., 2005. Regulation of myosin II during cytokinesis in higher eukaryotes. Trends in cell biology 15, 371-377.

Matsumura, F., Hartshorne, D.J., 2008. Myosin phosphatase target subunit: Many roles in cell function. Biochemical and biophysical research communications 369, 149-156.

Miki, H., Sasaki, T., Takai, Y., Takenawa, T., 1998. Induction of filopodium formation by a WASP-related actin-depolymerizing protein N-WASP. Nature 391, 93-96.

Miki, T., Smith, C.L., Long, J.E., Eva, A., Fleming, T.P., 1993. Oncogene ect2 is related to regulators of small GTP-binding proteins. Nature 362, 462-465.

Morita, K., Hirono, K., Han, M., 2005. The Caenorhabditis elegans ect-2 RhoGEF gene regulates cytokinesis and migration of epidermal P cells. EMBO reports 6, 1163-1168.

Newman-Smith, E.D., Rothman, J.H., 1998. The maternal-to-zygotic transition in embryonic patterning of Caenorhabditis elegans. Current opinion in genetics & development 8, 472-480.

Patel, F.B., Bernadskaya, Y.Y., Chen, E., Jobanputra, A., Pooladi, Z., Freeman, K.L., Gally, C., Mohler, W.A., Soto, M.C., 2008. The WAVE/SCAR complex promotes polarized cell movements and actin enrichment in epithelia during C. elegans embryogenesis. Developmental biology 324, 297-309.

Piekny, A., Werner, M., Glotzer, M., 2005. Cytokinesis: welcome to the Rho zone. Trends in cell biology 15, 651-658.

Piekny, A.J., Johnson, J.L., Cham, G.D., Mains, P.E., 2003. The Caenorhabditis elegans nonmuscle myosin genes nmy-1 and nmy-2 function as redundant components of the let-502/Rho-binding kinase and mel-11/myosin phosphatase pathway during embryonic morphogenesis. Development 130, 5695-5704.

Piekny, A.J., Mains, P.E., 2002. Rho-binding kinase (LET-502) and myosin phosphatase (MEL-11) regulate cytokinesis in the early Caenorhabditis elegans embryo. Journal of cell science 115, 2271-2282.

Piekny, A.J., Wissmann, A., Mains, P.E., 2000. Embryonic morphogenesis in Caenorhabditis elegans integrates the activity of LET-502 Rho-binding kinase, MEL-11 myosin phosphatase, DAF-2 insulin receptor and FEM-2 PP2c phosphatase. Genetics 156, 1671-1689.

Pohl, C., Tiongson, M., Moore, J.L., Santella, A., Bao, Z., 2012. Actomyosin-based self-organization of cell internalization during C. elegans gastrulation. BMC biology 10, 94.

Pollard, T.D., 2007. Regulation of actin filament assembly by Arp2/3 complex and formins. Annual review of biophysics and biomolecular structure 36, 451-477.

Pollitt, A.Y., Insall, R.H., 2009. WASP and SCAR/WAVE proteins: the drivers of actin assembly. Journal of cell science 122, 2575-2578.

Priess, J.R., Hirsh, D.I., 1986. Caenorhabditis elegans morphogenesis: the role of the cytoskeleton in elongation of the embryo. Developmental biology 117, 156-173.

Pruyne, D., Evangelista, M., Yang, C., Bi, E., Zigmond, S., Bretscher, A., Boone, C., 2002. Role of formins in actin assembly: nucleation and barbed-end association. Science 297, 612-615.

Ratheesh, A., Gomez, G.A., Priya, R., Verma, S., Kovacs, E.M., Jiang, K., Brown, N.H., Akhmanova, A., Stehbens, S.J., Yap, A.S., 2012. Centralspindlin and alpha-catenin regulate Rho signalling at the epithelial zonula adherens. Nature cell biology 14, 818-828.

Roh-Johnson, M., Shemer, G., Higgins, C.D., McClellan, J.H., Werts, A.D., Tulu, U.S., Gao, L., Betzig, E., Kiehart, D.P., Goldstein, B., 2012. Triggering a cell shape change by exploiting preexisting actomyosin contractions. Science 335, 1232-1235.

Sawa, M., Suetsugu, S., Sugimoto, A., Miki, H., Yamamoto, M., Takenawa, T., 2003. Essential role of the C. elegans Arp2/3 complex in cell migration during ventral enclosure. Journal of cell science 116, 1505-1518.

Severson, A.F., Bowerman, B., 2002. Cytokinesis: closing in on the central spindle. Developmental cell 2, 4-6.

Shakir, M.A., Gill, J.S., Lundquist, E.A., 2006. Interactions of UNC-34 Enabled with Rac GTPases and the NIK kinase MIG-15 in Caenorhabditis elegans axon pathfinding and neuronal migration. Genetics 172, 893-913.

Shakir, M.A., Jiang, K., Struckhoff, E.C., Demarco, R.S., Patel, F.B., Soto, M.C., Lundquist, E.A., 2008. The Arp2/3 activators WAVE and WASP have distinct

genetic interactions with Rac GTPases in Caenorhabditis elegans axon guidance. Genetics 179, 1957-1971.

Shelton, C.A., Carter, J.C., Ellis, G.C., Bowerman, B., 1999. The nonmuscle myosin regulatory light chain gene mlc-4 is required for cytokinesis, anterior-posterior polarity, and body morphology during Caenorhabditis elegans embryogenesis. The Journal of cell biology 146, 439-451.

Shoval, I., Kalcheim, C., 2012. Antagonistic activities of Rho and Rac GTPases underlie the transition from neural crest delamination to migration. Developmental dynamics : an official publication of the American Association of Anatomists 241, 1155-1168.

Simske, J.S., Koppen, M., Sims, P., Hodgkin, J., Yonkof, A., Hardin, J., 2003. The cell junction protein VAB-9 regulates adhesion and epidermal morphology in C. elegans. Nature cell biology 5, 619-625.

Smallhorn, M., Murray, M.J., Saint, R., 2004. The epithelial-mesenchymal transition of the Drosophila mesoderm requires the Rho GTP exchange factor Pebble. Development 131, 2641-2651.

Soto, M.C., Qadota, H., Kasuya, K., Inoue, M., Tsuboi, D., Mello, C.C., Kaibuchi, K., 2002. The GEX-2 and GEX-3 proteins are required for tissue morphogenesis and cell migrations in C. elegans. Genes & development 16, 620-632.

Sulston, J.E., Schierenberg, E., White, J.G., Thomson, J.N., 1983. The embryonic cell lineage of the nematode Caenorhabditis elegans. Developmental biology 100, 64-119.

Takai, S., Long, J.E., Yamada, K., Miki, T., 1995. Chromosomal localization of the human ECT2 proto-oncogene to 3q26.1-->q26.2 by somatic cell analysis and fluorescence in situ hybridization. Genomics 27, 220-222.

van Impel, A., Schumacher, S., Draga, M., Herz, H.M., Grosshans, J., Muller, H.A., 2009. Regulation of the Rac GTPase pathway by the multifunctional Rho GEF Pebble is essential for mesoderm migration in the Drosophila gastrula. Development 136, 813-822.

Vicente-Manzanares, M., Ma, X., Adelstein, R.S., Horwitz, A.R., 2009. Non-muscle myosin II takes centre stage in cell adhesion and migration. Nature reviews. Molecular cell biology 10, 778-790.

Williams-Masson, E.M., Malik, A.N., Hardin, J., 1997. An actin-mediated two-step mechanism is required for ventral enclosure of the C. elegans hypodermis. Development 124, 2889-2901.

Williams, B.D., Waterston, R.H., 1994. Genes critical for muscle development and function in Caenorhabditis elegans identified through lethal mutations. The Journal of cell biology 124, 475-490.

Withee, J., Galligan, B., Hawkins, N., Garriga, G., 2004. Caenorhabditis elegans WASP and Ena/VASP proteins play compensatory roles in morphogenesis and neuronal cell migration. Genetics 167, 1165-1176.

Wong, M.C., Schwarzbauer, J.E., 2012. Gonad morphogenesis and distal tip cell migration in the Caenorhabditis elegans hermaphrodite. Wiley interdisciplinary reviews. Developmental biology 1, 519-531.

Xu, Y., Moseley, J.B., Sagot, I., Poy, F., Pellman, D., Goode, B.L., Eck, M.J., 2004. Crystal structures of a Formin Homology-2 domain reveal a tethered dimer architecture. Cell 116, 711-723.

Zhang, H., Landmann, F., Zahreddine, H., Rodriguez, D., Koch, M., Labouesse, M., 2011. A tension-induced mechanotransduction pathway promotes epithelial morphogenesis. Nature 471, 99-103.

Zonies, S., Motegi, F., Hao, Y., Seydoux, G., 2010. Symmetry breaking and polarization of the C. elegans zygote by the polarity protein PAR-2. Development 137, 1669-1677.